Analysis of existing rockfall embankments of Switzerland (AERES) part A: state of knowledge

Stéphane Lambert, B. Kister

Analysis of Existing Rockfall Embankments of Switzerland (AERES)

Part A: State of Knowledge

Stéphane LAMBERT[1] and Bernd KISTER[2]

[1] Irstea, 2 rue de la papeterie, 38402 Saint Martin d'Hères cedex, France, + 33 4 76 76 27 94,
stephane.lambert@irtsea.fr
[2] Lucerne University of Applied Sciences and Arts, Technikumstrasse 21, CH – 6048 Horw, Switzerland.
Current position: kister - geotechnical engineering & research, Neckarsteinacher Str. 4 B,
D – Neckargemünd, +49 6223 71363, kister-ger@t-online.de

S. LAMBERT

Imprint

Commissioned by
Federal Office for the Environment (FOEN), Hazard Prevention Division, CH-3003 Bern.
The FOEN is an agency of the Federal Department of the Environment, Transport, Energy and Communications (DETEC).

Contractors
Lucerne University of Applied Sciences and Arts, CH-6048 Horw
Irstea, F-38402 Saint Martin d'Hères

Authors
Bernd Kister
Stéphane Lambert

FOEN support
Bernard Loup, Hazard Prevention Division
Arthur Sandri, Hazard Prevention Division

Notes
The AERES report consists of three parts:
- Part A: State of knowledge
- Part B: Analysis of the collected data and comparison with up-to-date knowledge
- Part C: Small-scale experiments

This study/report was prepared under contract to the Federal Office for the Environment (FOEN). The contractor bears sole responsibility for the content.

Suggested form of citation for Part A
Lambert S., Kister B. 2017: Analysis of Existing Rockfall Embankments of Switzerland (AERES); Part A: State of Knowledge. Federal Office for the Environment, Bern, 55 p.

Foreword

The aim of this document is to provide the reader with an up-dated and exhaustive vision of the worldwide knowledge concerning the design of rockfall protection embankments (RPE). As a definition, any structure in elevation of at least 2 m with respect to the ground, mostly made of granular materials (soil, gravel, …) and built with the aim of intercepting falling blocks are considered as RPE, whatever their cross sectional shape.

This state of the knowledge is based on different types of publicly available documents:
- National guidelines, recommendations and standards;
- Books;
- Journal articles, presenting a new approach, theoretically or applied to a case study;
- Conference communications, either presenting a new design approach or presenting a case study.

The document is intended for anyone with an interest in the design of RPE, whatever its level of expertise (contracting authority, owner, designer…). It is organized accordingly: the successive sections go from the basics to a discussion on the limitations of the available methods. The different design methods and previous research works are mentioned, making frequent references to existing documents for further reading.

Content

1. General context

As a definition, any structure in elevation of at least 2m with respect to the ground, mostly made of granular materials (soil, gravel, …) and built with the aim of intercepting falling blocks are considered as rockfall protection embankment[1] (RPE), whatever their cross sectional shape[2].

The very first references to RPE in the literature date back from the end of the 80's, even though the very first structures were built more than 50 years ago. Originally, RPE were mainly made from compacted natural soil and were designed for rather low-impact-energy events. Most often, their cross-sectional shape was trapezoidal. Sometimes, the uphill face was steepened for example with rockery or a concrete wall, gabions or prefabricated concrete components with the aim of increasing its steepness (Paronuzzi et al., 1989). At the end of the 1980s, ground-reinforced structures were developed to reach higher protection energies, higher than 100 MJ (Corté et al., 1989; Mathieu and Maréchal, 1989; Morino and Grassi, 1990).

Figure 1 Different types of RPEs (for authors, see Lambert and Bourrier, 2013)

---

[1] Also defined as rockfall control embankment in Austria (ONR, 2013)
[2] It thus also includes bunds and walls mentioned in CCC (2013) for example.

The variety of these structures has considerably increased over the last two decades, employing different types of construction materials (Figure 1). A descriptive comparison of some of these structures is given in Peila (2011). Many of these structures are presented in technical publications (Mathieu and Marchal, 1989; Morino and Grasso, 1990; Lazzari et al., 1996; Gerbert and Hespel, 1999; Mannsbart, 2002; Cargnel and Nössing, 2004; Coulon and Bruhier, 2006; Jaecklin, 2006; Rimoldi et al., 2008; Interreg III A, 2008; Brunet et al., 2009; Simmons et al., 2009; Hara et al., 2009; Lorentz et al., 2010; Broccolato et al., 2010; Grimod and Segor, 2014; Frenez et al., 2014…).

Table 1 lists the possible materials for the structure's uphill face, core and downhill face. Various combinations can be found between these three lists, some extremely rare and others common worldwide or found only in certain countries. For instance, in France interconnected soil-filled recycled tires are used as face material only or as both core and face materials. On the contrary, earth-dams with a rockery front face are frequently used in various countries (France, Switzerland…). Most often, the RPE is associated to a ditch, aiming in particular at collecting the blocks and fallen material volumes.

Most of the developments over the last decades concern soil-reinforced structures, using horizontal inclusions such as geosynthetics with the aim of increasing the RPE capacity and increasing the steepness of its uphill face while substantially reducing the volume of the structure as well as its footprint and visual impact.

Table 1 . Possible constitutive materials of rockfall protection embankments.

Uphill face	Core	Downhill face
Interconnected tires	Soil reinforced with GSY[1]	Gabion[2]
GSY[1]	Soil reinforced with interconnected tires	Soil
Metallic wire mesh	Soil reinforced with metallic wire mesh	GSY[1]
Cast iron panel	Soil reinforced with wood and steel	Tires
Gabion[2]	Soil bag[3]	Timber
Soil bag[3]	Gabion[2]	Rockery/rip-rap
Soil	Compacted soil	
Timber		
Concrete		
Rockery/rip-rap		

1. Geosynthetics, such as geotextiles or geogrids
2. Woven wire mesh (hexagonal) or welded wire mesh cages filled with either coarse or fine granular materials.
3. Typically a sand-filled geotextile sock.

RPE are appropriate when medium- to very-high-kinetic-energy events are expected, from a few hundred kilojoules to tens of megajoules. They are preferred over net fences when the design impact is higher than 5000 kJ (Descoeudres, 1997). The other declared advantages are low maintenance costs and reduced visual impact (Brunet et al., 2009). Nevertheless, they are not appropriate on steeper slopes and their construction generally requires extensive space and accessibility for heavy vehicles. For large structures, designed for high-kinetic-energy blocks, the ditch is dug in the slope uphill of the structure and the cut materials are generally used to erect the embankment.

In some cases, RPE are not intended to control the trajectory of medium to large kinetic energy single blocks, but to stop and contain frequent and limited kinetic energy rockfall or rockslides. In such cases, the accumulation of debris in the ditch dictates the structure design and requires planning debris removal when the maximum permissible volume is reached. Also, some embankments are designed to divert rockfall (Calvino et al., 2001; Interreg III A, 2006). These structures may either be dam-like or stem-like.
These cases are rather rare and not detailed in the literature.

The design of RPE addresses different issues, some being specific while others are more classical in the field of geotechnical engineering. These later are:
- Global stability of the slope: the slope stability may be altered as a result of an excessive RPE mass, or of the cut in the talus;
- Internal stability of the RPE, under static and seismic loadings;
- Interaction of the RPE with natural flows (surface run-off, torrent, debris flow, water source, snow avalanche), that may accumulate in the ditch, with possible detrimental influence on the RPE stability. (e. g., Gondo, Valais, in Jaecklin, 2006).

On the contrary, the design with respect to the block's trajectory and the structure's stability under impact are highly specific. These two facets of RPE design are referred to as the functional and the structural design, respectively. These two facets are developed in detail in the following, considering that classical facets are developed elsewhere.

2. Functional design

2.1. Introduction
As for any type of passive countermeasure against rockfall aiming at controlling the block trajectory, the functional design of RPE is based on trajectory analysis, which can provide a statistical distribution for the blocks passing height[3] and velocity in the vicinity of the RPE.

The ability of the RPE to act as a barrier against rockfall depends on its dimensions. It also depends on the ditch width: the larger the ditch the smaller the impact energy and passing height of the blocks reaching the embankment. As a consequence, there basically exist two

---

[3] Also refered to as jump height, flying height or bounce height in the literatue.

strategies concerning the design approach for the ditch-RPE system: (1) a catchment ditch made of loose material intended to dissipate the block's energy before it reaches the embankment (Peckover and Kerr, 1977; Hoek, 2007; Maegawa et al., 2011) or (2) a ditch made of a dust road allowing the circulation of heavy vehicles for fallen block removal, particularly in areas where frequent or large-volume events are expected. In the former strategy, the embankment, which represents the completion of the dissipative ditch, has a limited importance on the system efficiency as the ditch dissipates most of the incident kinetic block energy, with consequences on the impact conditions on the structure. Design charts have been proposed for the design of such ditch-RPE systems. For example, Figure 2 gives the values of ditch width (L) and ditch depth (D) with respect to the RPE crest for pairs of values of talus slope inclination (α) and block vertical travelling distance (H). In this example, the ditch width may be twice the height of the embankment, which may be less than 2 meters in height. For example, in case of a 30 m. in height slope with a 60° inclination, the ditch should be 4 m in width and 2 m in depth, approximately. This strategy will not be detailed in the following. Instead of that focus will be on large dimension structures exposed to severe loadings (later strategy).
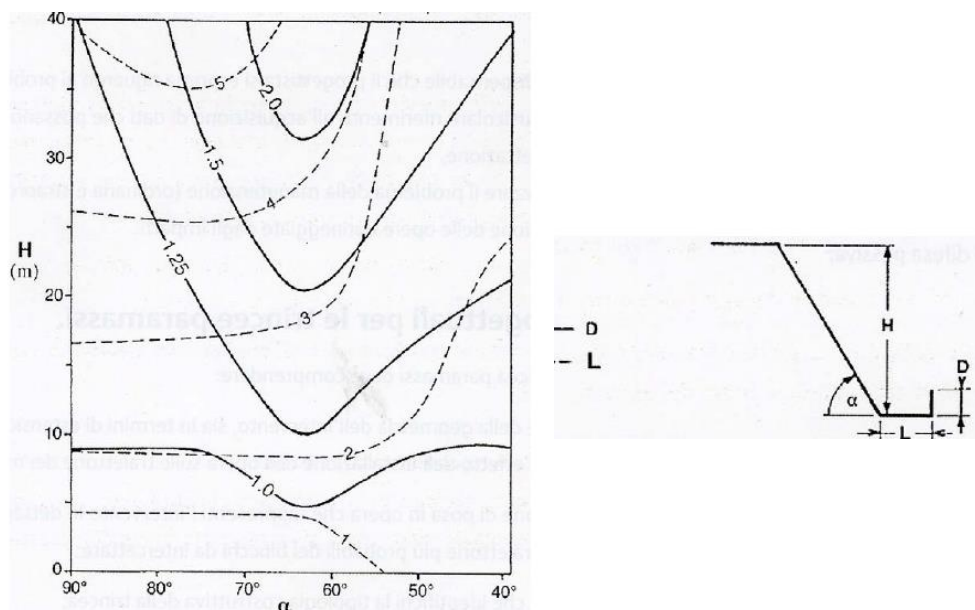
Figure 2. Example of design chart for catching ditches (Whiteside, 1986)

The functional design of a RPE aims at defining the structure geometry, which allows intercepting the blocks. This design is based on trajectory simulation data and aims at reducing the percentage of passing blocks below a targeted value. In general, this design is conducted after the RPE is positioned along the slope, after considering topographical or land-use constraints. Occasionally, the position of the embankment along the slope is defined with the aim of minimizing the block passing height and kinetic energy in the RPE vicinity, with positive consequences on the RPE dimensions.

The scientific and technical literature on the efficiency of RPE in controlling the block's trajectory is rather reduced. Some references address the efficiency of existing embankments in stopping the blocks, but with minimum details on the functional design method and criteria (e.g. Masuya et al., 2009, Agliardi and Crosta, 2003; Agliardi et al., 2009). Besides, some recommendations have been proposed in France (Calvino et al., 2001), Italy (UNI, 2012) and Austria (ONR, 2013). In such a context, the state of knowledge is presented considering successively the two main parameters governing the RPE ability in controlling the block trajectory, namely the structure height (section 2.2) and the uphill face inclination (section 2.3). Then, limitations of the proposed recommendations are discussed.

2.2. Structure height

The structure height is here defined as the distance along the vertical axis from the toe of the uphill face to the crest of the RPE (Fig. 3 a). This definition is consistent with most of the references, even if in some cases the height is referred to the direction perpendicular to the slope, to the structure face or to the vertical distance to the natural ground (resp. H', H'' and H''' in Figure 3 b). The definition for H' results from the fact, that the block passing height, provided by some trajectory simulation tools, is measured along the perpendicular to the soil surface.
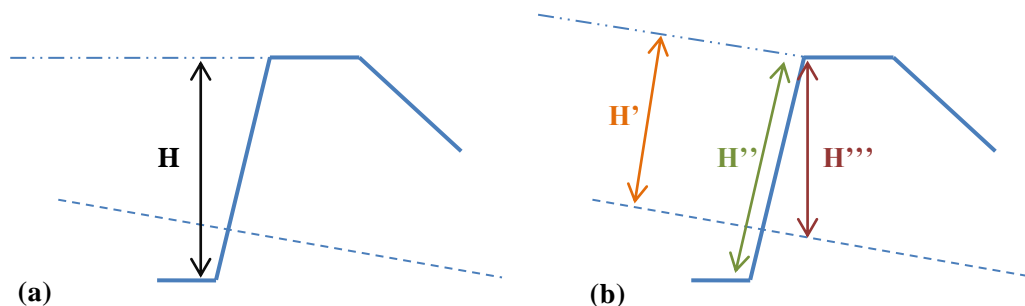
Figure 3 Structure height definitions: (a) as considered in this report and (b) other existing ones.

The RPE height should be determined based on the reference block's passing height increased by a freeboard.

In the majority of cases the reference block's passing height is defined based on statistics associated to the trajectory simulation results. In Italy and Austria, it is recommended to consider the 95% percentile of the passing height distribution (UNI, 2012; ONR, 2013). In addition, the Austrian standard considers the Eurocode principles and considers the block passing height multiplied by a safety coefficient varying from 1.05 to 1.3 depending on a consequence class, i.e. related to both the effect on the RPE and the elements at risks nature (Mölk and Hofmann, 2013).

The freeboard aims at avoiding impacts close to the crest, which can be highly detrimental to the structure efficiency. Indeed, an impact close to the crest leads to higher structure deformation, favouring the structure over topping or rolling over (Mölk and Hofmann, 2011; Breugnot et al., 2015). Also, blocks having a high rotational energy may roll over the RPE in case of an impact close to the crest (Kister, 2015).

Table 2 Recommendations for the minimum freeboard to consider, in different countries.

Country (réf.)	Recommended freeboard (min)	Context
France (Calvino et al., 2001)	Block radius*1	Radius of the largest expected block
Italy (UNI, 2012)	Block radius*1	
Austria[i] (ONR, 2013)	Block radius*2	Unreinforced RPE with rockery at the uphill face and an inclination of at least 50°
	Block radius*3	Reinforced RPE with a uphill face inclination less than 70°
	Block radius*2	Reinforced RPE with a uphill face inclination higher than 70°
	Block radius*4	Other embankments (made of compacted soil only)

i: see the paragraph below for the definition of the freeboard according to this standard

The recommended freeboard is generally expressed as a multiple of the block size. As shown in Table 2 it ranges from 1 to 4 times the block radius depending on the case. The freeboard considered by the Austrian standard is measured along the face of the RPE (in accordance with H'' in Figure 3), and not along the vertical axis. In addition, the Austrian standard considers the distance between the embankment crest and the top point of the block, and not its mass centre. Other references are not explicit on these points.

2.3. Uphill face inclination

In order to reduce the risk of rolling over, the steepness of the uphill face of the RPE should be increased. Rolling over may occur in case of a block rolling before reaching the structure and with a high rotational velocity or as a result of an impact close to the RPE crest, by a block with a high rotational velocity.

In France, a steepness of at least 65° is recommended (Calvino et al., 2001). Steeper inclinations are sometimes mentioned in specific studies (Simmons et al., 2009). The Austrian standard suggests a steep face and recommends freeboard depending on the face steepness.

2.4. Comments on these recommendations

Table 2 reveals that the required structure height is different depending on the text considered, for given block radius and passing height. The freeboard along the vertical axis based on the Austrian standard is at least 2.5 times higher than that when considering other recommendations, with a maximum up to 4 times. This will lead to huge differences in

structure height and volumes, in particular when dealing with large blocks, and will probably make some projects unfeasible for costs, available place and natural slope stability reasons.

These recommendations were proposed based on empirical knowledge, except for the Austrian ones. In this latter case, small scale experiments were conducted in the lab (Hofmann and Mölk, 2012), considering RPE varying in size and construction type. Globally, there are only a few research works addressing the influence of the geometrical characteristics of the RPE and of the block kinematics prior the impact on the functional efficiency of RPE. Existing ones are rather recent (Plassiard and Donzé, 2009; Toe et al., 2013; Kister, 2015) As a consequence, neither the inclination of the block incident trajectory nor its rotational velocity is considered for the functional design (the Austrian standard introduces this parameter for structural design purpose only, without any indication about the statistic estimator to consider).

In terms of incident trajectory, evidences from the field showed that a block with an upward incident trajectory could over top a vertical face RPE after an impact more than one block radius from its crest (Figure 4). In this case, it was favoured by the large deformation of the RPE facing as a result of the impact.

Figure 4 This 3-m-tall gabion embankment was cleared by a block after an impact more than 1 m below its crest, by a block having an upward incident trajectory (Ste Marie de Cuines (73), France).(S. Lambert)

The rotational kinetic energy is often neglected because it is generally less than $10 - 15\%$ of the total block energy (Chau, et al., 2002; Bourrier and Hungr, 2011). Numerical simulations have suggested that both the block rotational velocity and trajectory inclination have a strong influence on the ability of the block to roll over the RPE while considering a freeboard as large as 0.8 times the block diameter (Plassiard and Donzé, 2009). The influence of the rotational energy has been confirmed by small-scale tests (Kister, 2015; Figure 5), even for low rotational energies. This is even more pronounced in case of low uphill steepness face values.
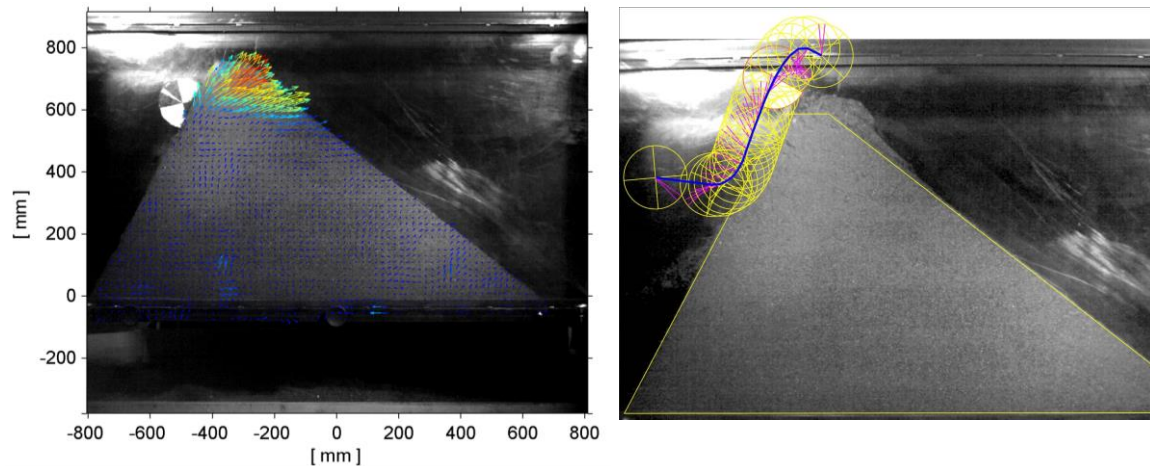
Figure 5 Quasi-2D small scale experiments showing high displacement fields at the crest (left) and over topping of structure by the block resulting from a high rotational energy (right) (Kister et al., 2014).

Thanks to real scale field tests Clerici et al. (2013) showed that the movement of a bloc rolling towards the embankment crest could be significant. The tested embankment was 3 m. in height, with a crest thickness of 1.7 m. The structure was reinforced with geosynthetics and exhibited an uphill face angle of 71°. The embankment was impacted by a sphere (diameter 1.5 m) rolling down the natural slope, with velocities between 10 m/s and 15.75 m/s. The upward movement of the sphere along the embankment face during the impact was up to 1.5 m.

While trajectory simulation results are of paramount importance for the design of RPE, no specific recommendations are proposed for a proper use of these tools.

Some recommendations suggest considering the 95% percentile of the block passing height for defining the structure height. This suggestion leads to the following comments:

- This percentile is less dependent on the simulation number than the 99% percentile or the maximum. Nevertheless, there is no requirement in terms of minimum number of block reaching the RPE required for obtaining a reliable 95% percentile of the passing height, while this value is sensitive to the number if less than 1000, at least.
- A distinction between 2D and 3D tools in terms of passing height statistics, should be made, in particular because, the latter case requires a higher number of simulation and the definition of the way to establish statistics depending on the digital model elevation resolution (Lambert et al., 2013).
- Except for the Austrian recommendations, there is no indication on the block point to consider for determining the block passing height, and consequently the RPE height. This may lead to confusion, as trajectory simulation tools either consider the block lower point, or the block mass centre.

None of the recommendations explicitly requires conducting the simulation in the presence of the embankment, i.e. accounting for the modified slope profile and for the ditch digging in particular. These significant changes strongly influence the block trajectory and should be accounted for.

In a similar mode, none of the recommendations suggest conducting simulations for estimating the effective residual risk on the new profile to assess the projected structure's efficiency in stopping the blocks. The residual risk depends on the occurrence of quite rare to extremely rare events resulting in embankment overtopping. For instance, if the 95% percentile is considered as design criteria, such cases may result from an unexpected reaction of the RPE to impact by a block within the 0-95% range, outliers in the 95-100% range or events related to scenarios not considered for the design (in terms of return period for instance). These critical cases, whose identification globally requires a large number of trajectory simulations, are characterized by large passing heights, high energies or high rotational velocities in the vicinity of the embankment.

Besides, the correct simulation of these critical and rare trajectory cases faces the limitations of the trajectory analysis tools, in particular in the embankment vicinity. In the embankment vicinity, the impact orientation is quasi-normal to the impacted surface, and coupling between the translational velocity and the rotational velocity may dramatically change the reflected block trajectory. This context thus differs from more classical trajectory analysis contexts for which parameters were calibrated (Lambert et al., 2013). The coupling between the translational velocity and the rotational velocity as well as the shape of the block are generally roughly accounted for in these models event though they seem to play an important role in the block's trajectory (Chau et al., 2002; Usiro et al., 2006). Toe et al. (2013) conducted small scale experimental tests with a sphere, a cube and a parallelepiped that were dropped on a slope terminated by an embankment. The block trajectory was modelled using two techniques (probabilistic and discrete element method). It was shown that approximately 40% of the spheres had been able to surmount the embankment, while no cube and no parallelepiped had passed the embankment in the tests (Figure 6).
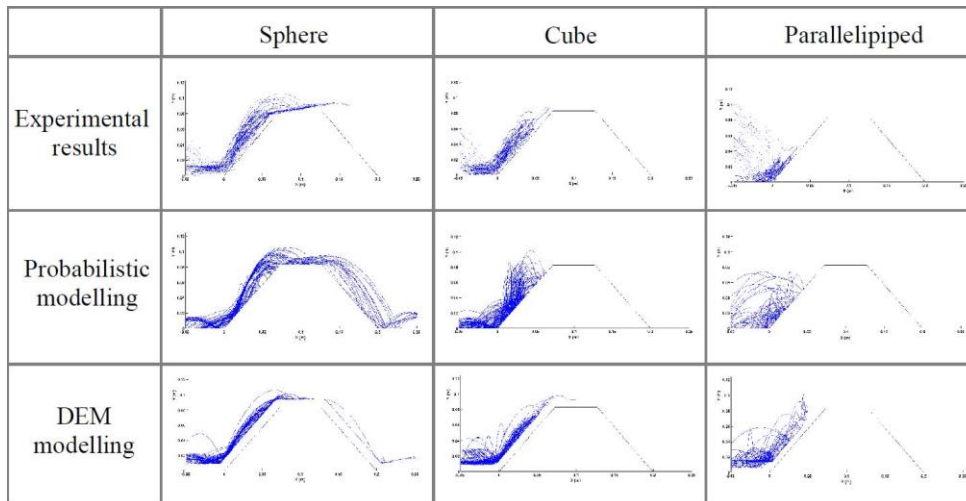
Figure 6 Experimental and simulated trajectories for three different block shapes (Toe et al., 2013).

Also, the spatial resolution of trajectory analysis tools may not be appropriate to satisfactorily account for the slope profile in the vicinity of the embankment, mainly for 3D codes (Lambert et al., 2013). Basically, a raster digital elevation model with a resolution of 2 m cannot reproduce the rapid slopes changes observed in the ditch and at the embankment.

As a consequence, particular care must be taken to satisfactorily model the trajectory of a block in the embankment vicinity with the aim of evaluating its efficiency in reducing the risk

Last, these recommendations concern RPE build to stop single blocks and not rockslides neither than successive and frequent rockfall. In such cases, the volume of solid material to contain in the ditch should be considered for defining the structure height. In the case of successive and regular rockfall, the height of the RPE should be the sum of the maximum permissible thickness of deposited material, the block passing height and freeboard.

3. Structural design

The impact of a block, whose typical velocity ranges from 5 to 30 m/s and whose mass ranges from a few to tens of thousands of kilograms, results in a dynamic localized loading lasting between 0.03 and 0.2 s and generating strain rates in the impact direction higher than 0.1 s−1. The design of earth-structures, such as RPE, exposed to such a specific dynamic loading confronts the engineers with

  i.   the large and irreversible deformations induced,
 ii.   the nonlinear soil stress-strain behaviour, and
iii.   the interaction between the different components of the structure (reinforcing components and soil).

As a consequence and by contrast with the functional design, the design with respect to impact has been addressed through many research works.

In the following, these works are briefly mentioned to analyse the embankment response. Then the available design methods are described and their limitations are discussed. Specific sections are dedicated to the today's only existing standards (UNI, 2012; ONR, 2013).

3.1. Specific research

The increasing need for efficient protection structures against high-energy block impacts has motivated research for more than 30 years. These are based on experimental, analytical and numerical developments. The main experimental research is presented in the following subsections.

3.1.1. Small-scale experiments

The first experiments were conducted in the 1980s in view of constructing a huge embankment with a 200-MJ capacity based on small-scale structures (Corté et al., 1989; Lepert and Corté, 1988). The 1/100 scale embankments made of sand were exposed to centrifuge impact tests at a 100-g acceleration (Figure 7). The impact force and acceleration within the embankment were recorded. In practice, these experiments confirmed that the planned RPE (7.2 m high and 800m long) would be effective against a 200-m^3 volume block with a velocity of 26 m/s.

The Technical University of Vienna also conducted small-scale experiments with the main objective of investigating the influence of the geotextile (Blovsky, 2002 and 2004; Brandl and Blovsky, 2004). Twenty model tests were carried out on embankments scaled at 1:50. The parameters investigated were the soil compaction, the uphill face steepness and the geotextile layout. Embankments with and without geotextiles were tested (Figure 8). In the former, different geotextile anchoring lengths were considered, also considering geotextile wrapping on both faces. Impacts were repeated several times, measuring the impact force. Comparisons were made based on the sum of impulses after three successive impacts by an instrumented pendulum used as impactor.

In Austria again, Hofmann and Mölk (2012) conducted small scale experiments (1-g) on structures varying in type and size while varying the impact conditions (Figure 9, Figure 10). The impactor was a steel sphere. The embankments were either made of sand only, sand and rip-rap face, or reinforced sand. Based on the results of the numerous experiments conducted, the authors proposed the basic essentials of the Austrian standard-guidelines for the design of RPE (ONR, 2013, see section 3.6).
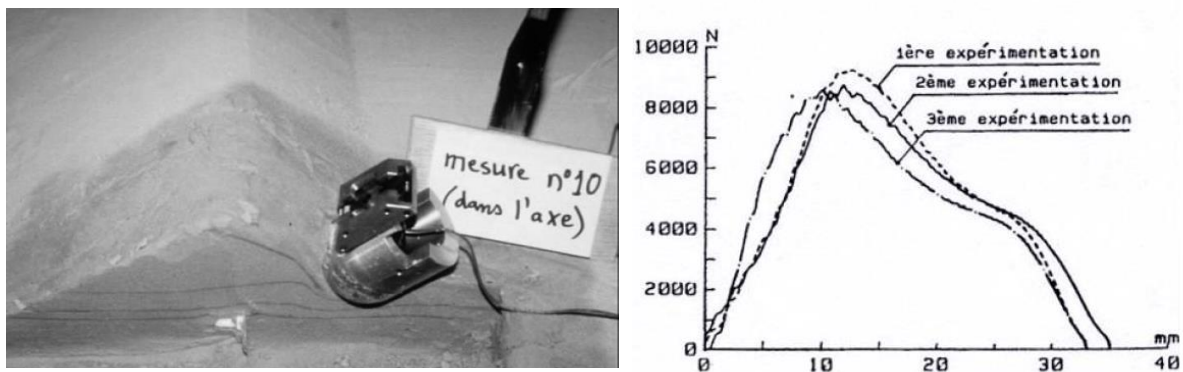
Figure 7 Centrifuge impact tests on an embankment conducted in France in the 1980's: impact embankment and impact force measurements (Lepert and Corté, 1988)

Figure 8 Post-impact top views of small-scale embankments showing the influence of the geotextile on the downhill face deformation: without/with geotextile, left/right (from Brandl and Blovsky, 2004).

Figure 9 Small-scale experiments conducted by Hofmann and Mölk (2013). Left: impact on an unreinforced structure. Right: reinforced structure after two impacts.

Figure 10 Illustration of the variety of embankment type and geometry and loading conditions in the small-scale experiments conducted by Moelk and Hofmann (2012).

Figure 11 Displacement field at 4 ms, 10 ms, 18 ms and 36 ms observed by Kister (2015).

More recently, small scale and half scale experiments were conducted at Lucerne University of Applied Science and Arts, in quasi-2D respective 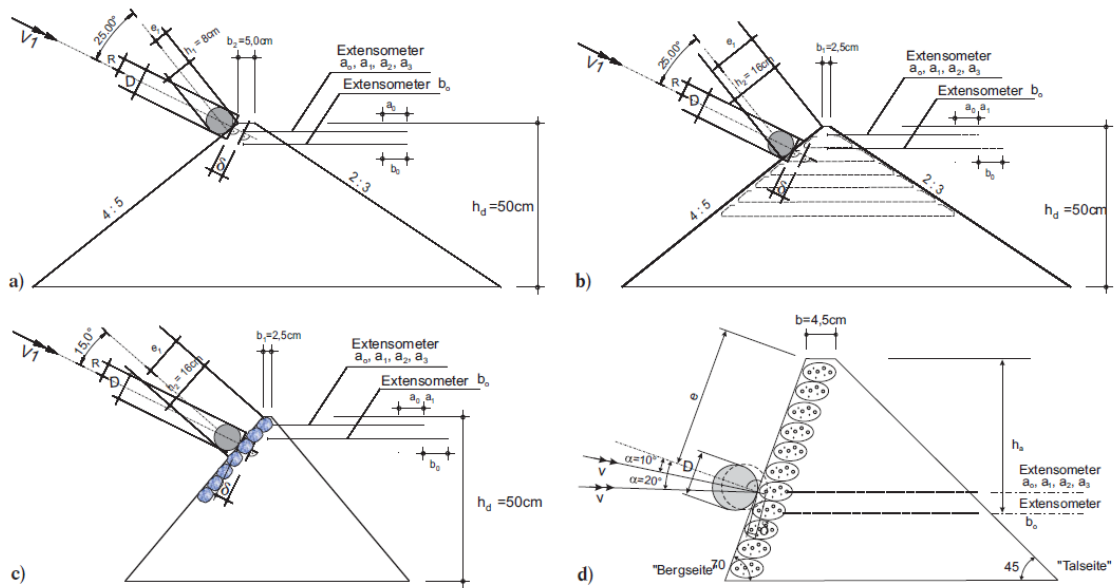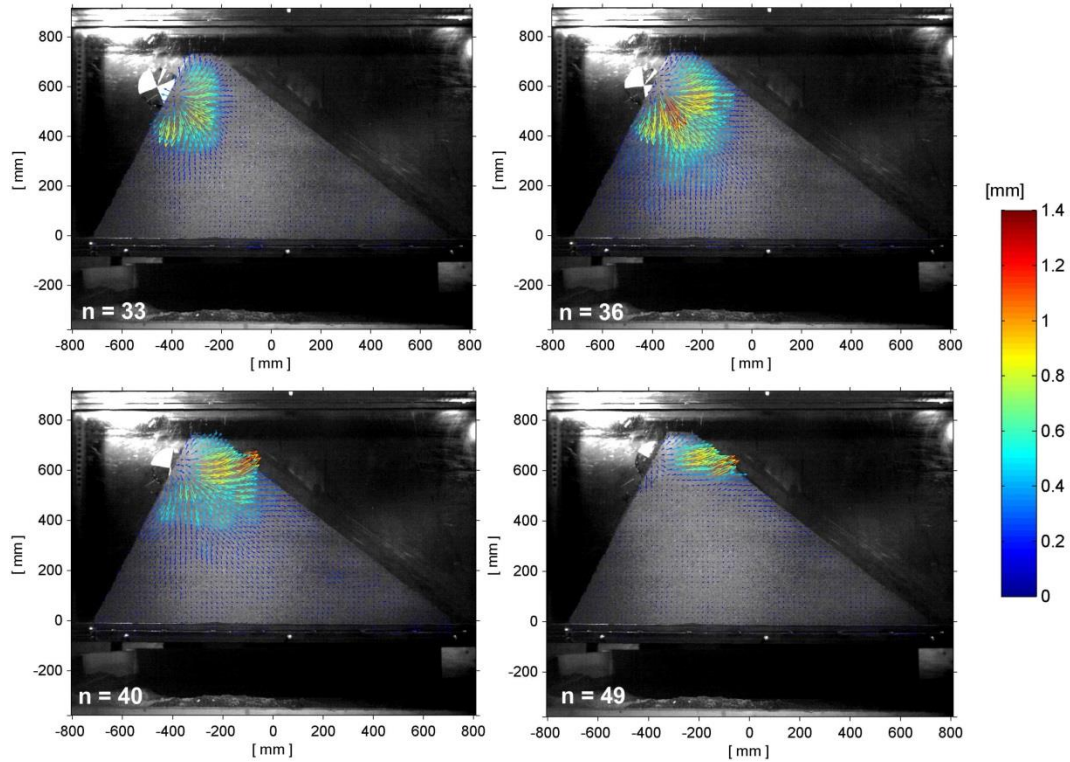in 3D conditions (Kister et al., 2014; Kister, 2015). Particle Image Velocimetry (PIV) allowed tracking over time of the displacement field inside the embankment. Additional the impactor's trajectory had been determined in the quasi-2D-tests (Figure 11). Embankments, differing in cross-section geometry (symmetric/asymmetric) and in crest width, were impacted by 6 different projectiles, differing by their shape, volume and unit mass. These experiments in particular showed the influence of the block rotational energy, block shape, block material and impact point location on the embankment deformation and for overtopping.

Small-scale experiments constitute a cost-saving alternative to real scale experiments, in particular with the aim of conducting parametric studies. The obtained results are of great qualitative value. Nevertheless, questions related to scaling issues and the extrapolation of results to the real scale may rise. This is particularly true for small scale tests under gravity, and less for centrifuge tests. On the other hand centrifuge tests are usually based on very small models because of the limited place in the centrifuge and so very often a realistic relationship of grain-size distribution of the RPE material and the RPE dimensions is not given.

3.1.2. Real scale experiments

The first real-scale impact experiments involved a structure type developed by the Colorado Department of Transportation in view of ensuring safety along an important road through a canyon (Burroughs et al., 1993; Hearn et al., 1995, 1996). The tests concerned a structure made of soil reinforced with geosynthetics, 24 m long, 3 m high and either 1.8 or 2.4 m thick, with vertical sides (Figure 12). Eighteen rock blocks of different shapes and masses were rolled down a hill against the barrier. The maximum block energy before the impact was 1400 kJ. The downhill face deformation increased nonlinearly with the boulder's kinetic energy, following a power law (Hearn et al., 1996). It decreased with the structure thickness: for a 1400-kJ impact, this deformation was 0.75 m and 0.35 m for a 1.8-m- and 2.4-m-thick structure, respectively (ref. A1/A3 in Table 3).

In the end of the 1990s, the behaviour of a new type of structure was investigated through real-scale experiments (Yoshida, 1999). This structure consisted of a soil-reinforced earthwork protected by two layers of soil bags, placed uphill (Figure 13). The soil bags were exposed to the impact to act as an energy dissipater to reduce the impact force on the reinforced embankment. Blocks were rolled down the hill, resulting in impact energies ranging from 58 to 2500 kJ (ref. C1/C3 in Table 3). All the blocks were stopped without a collapse of the structure. The deformation on the uphill face was measured. More recent experiments were conducted on similar structures, but no significant data is available (Protec Engineering, 2011).
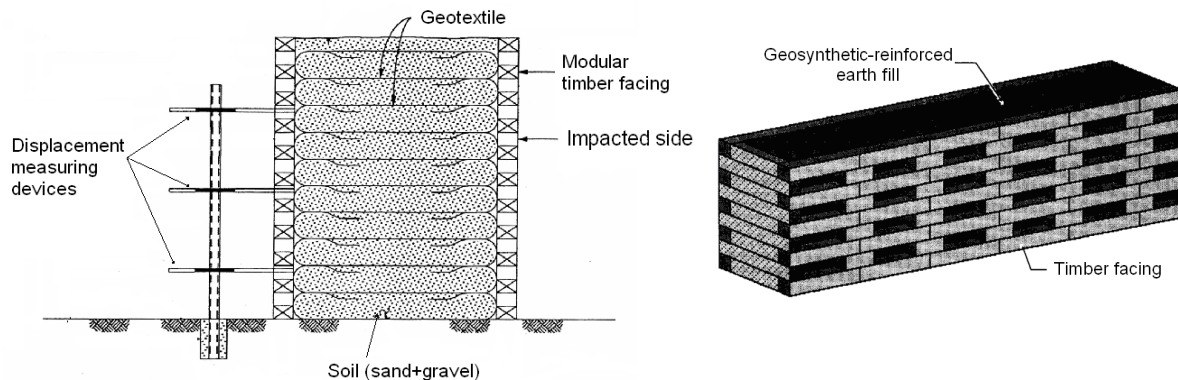
Figure 12 Structure tested by the University of Colorado (adapted from Burroughs et al., 1993; Hearn et al., 1995)
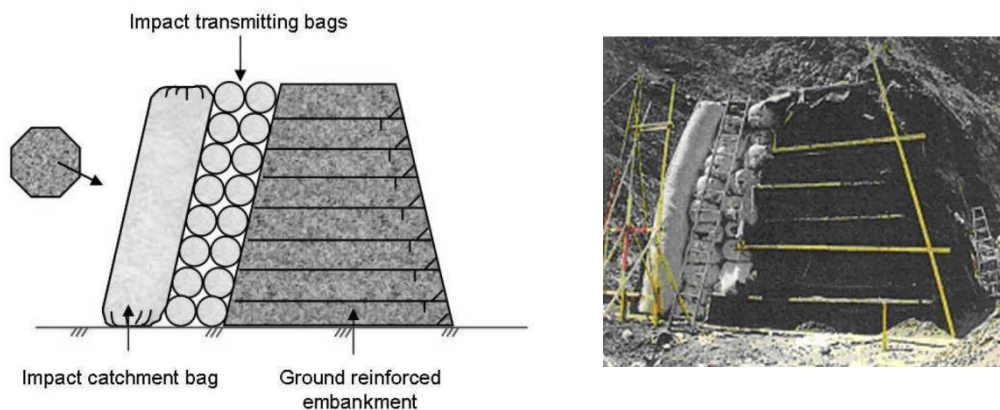
Figure 13 Embankments tested by Yoshida (1999).

Since the end of the 1990s, an important study has been conducted by the University of Torino on geosynthetic reinforced embankments (Peila et al., 2000, 2002, 2007, 2011; Ronco et al., 2009). Real-scale structures were tested on a site dedicated to rockfall protection structure testing (Figure 14). The equipment can convey blocks up to 10 tons at a velocity of 30 m/s. The blocks had almost no rotation when hitting the structure. A total of eight impact tests on five different embankments were performed. The impacted structures were reinforced with geosynthetics, except for one structure that was made of compacted soil (ref. B1 to B3 in Table 3). The parameters investigated were the geosynthetic type, the soil type and the block mass.

These reinforced embankments were demonstrated to be efficient against successive 4500-kJ impacts. This research is the most exhaustive work on the topic to date, including experiments and numerical modelling aiming to develop both design charts and numerical tools to be used for design purposes (Brunet et al., 2009; Ronco et al., 2010, Grimod and Giacchetti, 2013) and allowing back analysis of natural impacts (Peila, 2011).

In Japan, three real-scale structures differing in their construction materials were exposed to impacts (Sung et al., 2008; Aminata et al., 2009). Impact tests were either performed rolling blocks down a 17 m high hill or using a boulder suspended from a crane released from a height of 11 m, reaching a maximum energy of 110 kJ. The impacted structures were a geogrid-reinforced wall, 2 m high, and two walls made of ductile cast iron panels containing boulders (Figure 15). Block penetration, block velocity and impact force were derived from the measurement of block acceleration.
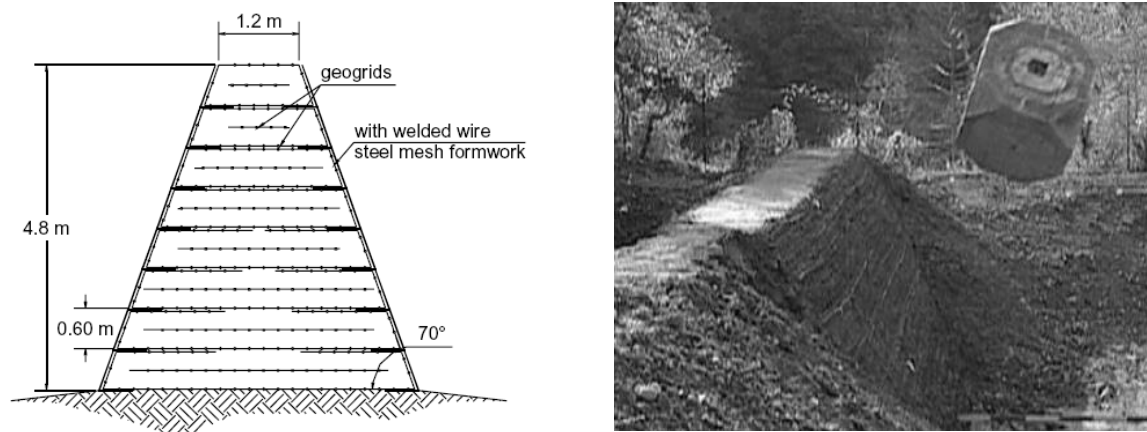

Figure 14 Embankments tested by the University of Torino (Peila et al., 2002).

Table 3 Some experimental data concerning impact experiments with energies higher than 1000 kJ.

Ref.	Structure Type	Height (m)	Thickness (crest/base) (m)	Block Mass (kg)	Translational Veloc. (m/s)	En. (kJ)	Impact Height (m)	Deformation Uphill-side (m)	Downhill-side (m)
A1	MSE wall	3.05	1.82	5300	19.5	1010	1.5	0.6	0.2
A2	+ wood[1]	3.05	1.82	8300	18.3	1400	1.4	0.9	0.7
A3		3.7	2.4	8400	18.3	1410			0.34
B1	Reinforced[2]	4.2	0.9/5	5000	31.7	2500	3	0.6	0.23
B2		4.2	0.9/5	8780	31.3	4350		1	0.9
B3	Unreinforced[2]	4.2	0.9/6	8780	31.3	4350	3	1.5	collapse
C1		4	3.3/5.3	3300	24	970	2	0.22	0
C2	GeoRockwall[3]	4	3.3/5.3	7700	24	2000	2-3		0.09
C3		4	3.3/5.3	17000	17.7	2700	3-4		0.5
D1	MSE wall +	4.2	2.2/4.3	10100	15.7	1243	2.31	1.56	0.266
D2	Geocell	4.2	3/5.1	17100	13.9	1567	2.85	1.44	0.091
D3	face[4]	4.2	2.2/4.3	17100	14.4	2037	2.55	1.73	0.239
E1	Gabion	3	3/11	6500	18	1040	2.1	0.42	0
E2	face+dam[5]	3	3/11	6500	26	2200	2.1	0.71	0

(1) Hearn et al., 1996; (2) Peila et al., 2002, 2007;(3) Yoshida et al., 1999; (4) Maegawa et al., 2011; (5) Lambert et al. (2014).

Maegawa et al. (2011) investigated the concept of sandwich structures as pioneered by Yoshida (Yoshida, 1999). The impacted structures differ in the structure's face, which is composed of geocells filled with gravel instead of soil bags. Impacts ranging from 786 to 2709 kJ were obtained by rolling a block down a 37-m-high slope onto the structure. Eight tests were performed on two types of structure. Deformation on the uphill face and the block acceleration were measured (ref. D1 to D3 in Table 3). All blocks were stopped.

Cellular rockfall protection structures have recently been investigated by Heymann et al. (2010) and Lambert et al. (2014). These structures are made of gabion cages filled with different materials depending on their location in the structure. The aim was to reduce the stresses transmitted within the structure by increasing the diffusion of stress as well as dissipation of the impact energy. In this purpose, shredded tires were used after demonstrating their limited environmental impact (Hennebert et al., 2014). Both half-scale and real-scale structures were impacted (Figure 16). Different fill materials were considered, including shredded tire–sand mixtures and ballast. Three different real-scale structures were subjected to an impact by a 6500-kg spherical boulder, with a maximum velocity of 25 m/s (ref. E1 and E2 in Table 3). Measurements in particular concerned accelerations of the boulder and within the structure, the transmitted forces and the structure deformations. Large deformation was observed in the structure. Figure 17 shows that velocities higher than 3 m/s were reached at a 1 m distance from the impacted surface, over a short period of time, and that compaction and loosening were observed after the impact up to 4 m from the impact point.
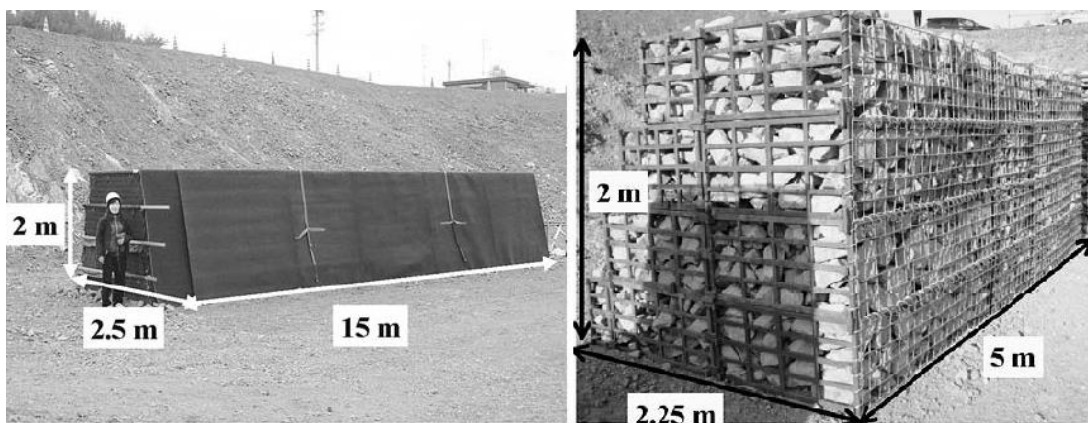
Figure 15 Two of the three structures recently investigated in Japan (Sung et al., 2008; Aminata et al., 2009).
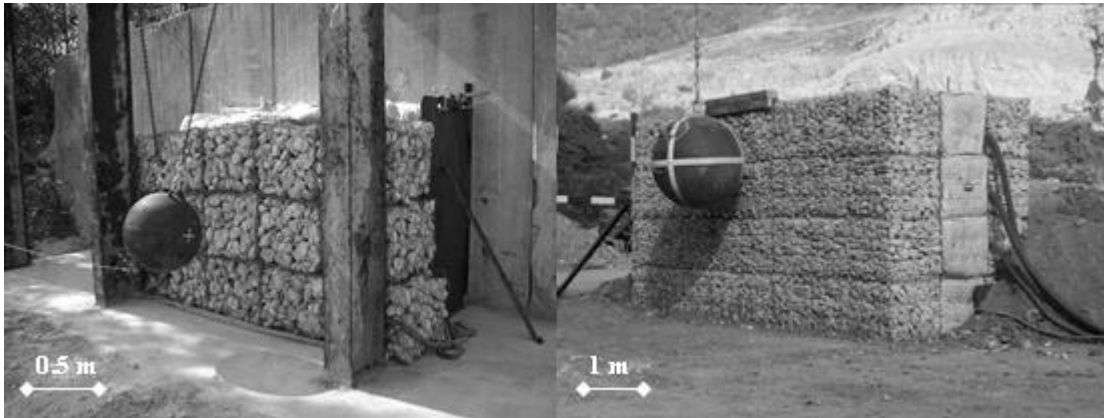
Figure 16 Half-scale and full-scale structures tested by Heymann et al. (2010) and Lambert et al. (2014).
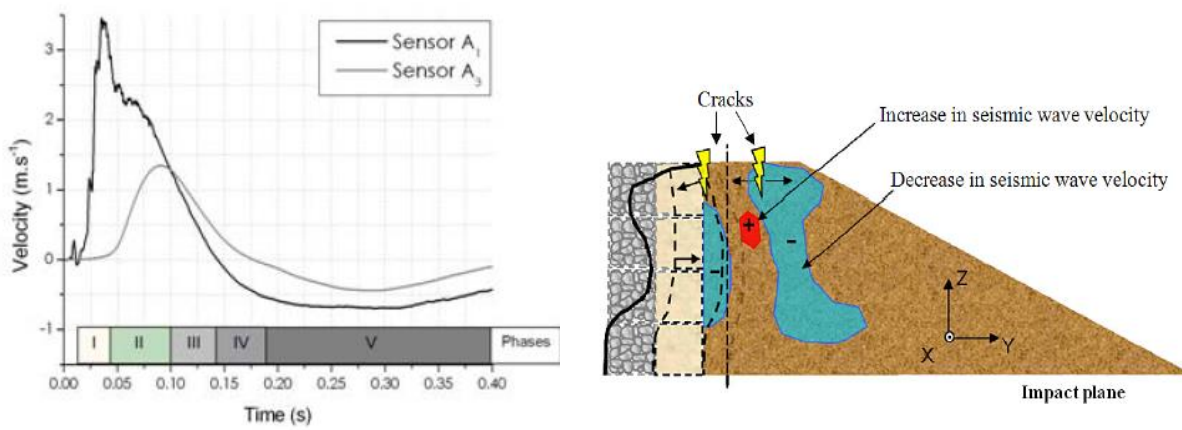

Figure 17 Velocities measured within the RPE at 2 distances from the impact point (left) and post-impact observations (Lambert et al., 2014)

Figure 18 Experiments conducted by Clerici et al. (2013)

Figure 19 6600 kJ impact experiment conducted by Mongiovi et al. (2013)

More recently, real-scale impact experiments were conducted in Italy, by the University of Brescia (Clerici et al. 2013) and by the University of Trento (Mongiovi et al., 2014). The former was conducted impacting a reinforced RPE by spheres rolling down a slope and developing energies up to 0.8 MJ (Figure 18). The latter also concerned a reinforced RPE, 4.8 m high, but with impact energies of almost 7 MJ, the highest ever reached in real scale experiments (Figure 19). In both cases, the block velocity was measured and the post-impact structure deformation was monitored by laser scan. In addition, experiments conducted by the University of Trento involved acceleration measurements within the RPE. Nevertheless, only limited data are available on these two experimental works.

3.1.3. Numerical approaches

As a complement to experimental investigations, various numerical models have been developed. Some were developed in parallel to the real-scale experiments, and rather fair agreements were obtained. The aim with some of these tools was to extend the study of the RPE response to higher impact energies than in the experiments (Ronco et al. 2009) or for addressing the influence of the block kinematics (Plassiard, 20007, Plassiard and Donzé, 2009; Murashev et al., 2013, Breugnot et al., 2015). The Finite Element Method (FEM) had been used by Burroughs et al. (1993), Peila et al. (2002, 2007), Sung et al. (2007) and Murashev et al. (2013). FEM-based approaches require an explicit method and a re-meshing algorithm taking rockfall dynamics into account and modeling large deformations (Peila et al., 2007). The Finite Difference Method (FDM) has been used by Jarrin and Meignan (2010). On the contrary, the Discrete Element Method (DEM) is based on Newton's equation of motion and naturally allow modelling large deformations. DEM-based approaches have been used by many authors (Hearn et al., 1995, 1996; Carotti et al., 2004; Nicot et al., 2007; Plassiard and Donzé, 2009, 2010; Bertrand et al., 2010; Bourrier et al., 2011; Lorentz et al., 2010). Breugnot et al. (2015) have proposed the use of a combined discrete-continuum approach in order to derive advantages of the discrete approach in the impact area and of the finite element approach in the far field. They investigated the influence of the block shape, impact location and the ratio of mass to velocity for a same kinetic energy.

Even if allowing conducting parametric studies, the numerical models are mainly research oriented, because they are complex, require specific skills and the calculations are time consuming. To some extent, these models are out of reach for most of the design companies. As an illustration, the literature is extremely poor in terms of application of such models to specific study cases (Lorentz et al., 2010; Murashev et al., 2013). Last, these models are mainly used by their developers and are not accessible for their reliability to be evaluated.

Consequently, these numerical works won't be addressed in details but reference to some of these will be made in the following sections, when relevant.

Despite the great variability of testing conditions and structure types, real-scale experiments globally provide a valuable database for investigating the response of RPE to block impact. Table 3 reports some experimental results obtained on real-scale structures with impact energies higher than 1000 kJ. The capacity of the embankment, in terms of the impact energy it can withstand without collapsing, is the most important information obtained. The analysis of the response of impacted structures may also be based on the residual deformation on both uphill and downhill faces of the embankment after an impact. In particular, the downhill face deformation can be considered as a simple design criterion, because it governs post-impact structure stability (Ronco et al., 2009).

3.2. What can be learned about the response of an embankment to block impact?

The different published works presented in the previous section, and involving real-scale and small scale experiments as well as numerical modelling, gives elements for describing the response of a RPE to a block impact and helps to understand the main mechanisms involved.

The response of the RPE to impact, until collapse, may be described as a three-phase process, as proposed by Lambert and Bourrier (2013) (Figure 20).

When the block starts penetrating the RPE, a high stress is generated in the vicinity of the impacted area, with peak values higher than 1 MPa (phase 1). The increase in stress leads to the compaction of granular materials with possible particle crushing, depending on the embankment fill material characteristics: the narrower the soil grading, the larger the particle size and the higher the stress, the greater the chance of grain crushing.

The rest of the structure exhibits almost no significant changes. It basically acts as a buttress allowing compaction and particle crushing on the uphill face.

The very high stress gradient, which expands from the uphill face to the downhill face of the RPE induces displacement of the grains locally. A displacement field appears in the stressed zone. This displacement field has a tendency to move upward while going through the structure (Lambert et al., 2013; Kister, 2015).
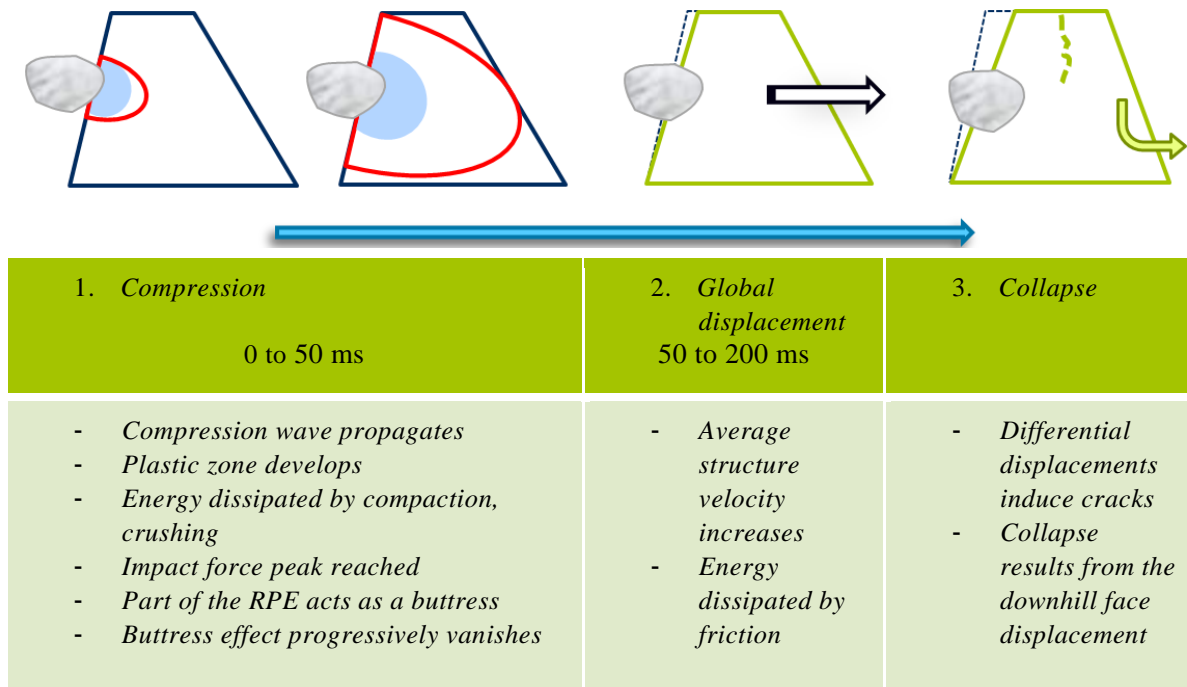
1. *Compression* 0 to 50 ms	2. *Global displacement* 50 to 200 ms	3. *Collapse*
- *Compression wave propagates* - *Plastic zone develops* - *Energy dissipated by compaction, crushing* - *Impact force peak reached* - *Part of the RPE acts as a buttress* - *Buttress effect progressively vanishes*	- *Average structure velocity increases* - *Energy dissipated by friction*	- *Differential displacements induce cracks* - *Collapse results from the downhill face displacement*

Figure 20 A 3-phases schematic description of the RPE response to impact, until collapse (Lambert and Bourrier, 2012).

Progressively, the front of the stressed volume moves within the RPE and, concomitantly, the buttress effect vanishes with time. The amplitude of the stress peak decreases with the travelled distance, due to both geometrical and material attenuations. After a given period of time and especially for slender constructions, the displacement field may involve the whole RPE cross-section (phase 2). Indeed, as the downhill face is a free boundary, the stress increase results in a downhill-oriented movement of this face. The displacement then concerns a volume with lateral extension higher than twice the block diameter (Blovsky, 2002, 2004; Peila et al., 2007; Hofmann and Mölk, 2013; Lambert et al., 2013; Kister, 2015). Besides, the displacement is more pronounced closed to the crest than at the RPE base, where no displacement is observed. This displacement of part of the RPE leads to dissipation by friction, along shear planes developing through the structure.

Finally, if the stress increase close to the downhill face is high enough, soil loosening and bulking may occur on the downhill face as well as on the crest (phase 3) (Blovsky, 2002, 2004; Hofmann and Mölk, 2013; Lambert et al., 2014; Kister, 2015). Cracks parallel to the face may develop within the structure as a result of these displacements (Peila et al., 2002; Lambert et al., 2014, Kister, 2015). The structure finally may collapse, as a result of the downhill face large displacement.

The occurrence and magnitude of the different mechanisms mentioned depend on the impact energy in proportion to the embankment's capacity to absorb energy.
For low impact energies, both the penetration required to stop the block and the stress generated within the embankment are small (ref A1, B1, C1 in Table 3). The residual downhill

face deformation is small compared to the block penetration. The impact energy is dissipated by compaction and grain crushing in the vicinity of the impact area while only a small part propagates by elastic waves. In such as situation, there is neither phase 2 nor a phase 3.

With a higher impact energy, both the block penetration and stress within the embankment increase. The volume of material undergoing plastic strains increases, similar to what is observed for ground compaction (Mayne and Jones, 1983). The downhill face displacement increases and for slender structures, the displacement may progressively tend toward the value of the uphill face displacement (e.g., ref. A1 and A2 in Table 3). Nevertheless, the thicker the embankment, the lower is the downhill face displacement (e.g., ref. D1, D2, E1 and E2 in Table 3).

Dissipative mechanisms depend on the time considered and on the position in the structure. Compaction is predominant close to the impact, at the impact beginning. At far distance from the impact, compaction is much less because of the spatial energy attenuation of a "point load", which is in inverse proportion to the distance. On the contrary, energy at larger distance from the impact and for larger times may be dissipated along shear planes developing as a result of the structure displacement. Overall energy dissipation through soil compaction remains predominant during the impact process, with an estimated proportion of about 75 to 80% of the block's kinetic energy (Ronco et al., 2009, Kister and Fontana, 2011).

The structure's response versus time thus reveals the influence of the different parameters related to the material characteristics: the parameters associated with their compressive response, friction angle and unit mass. The influence of these parameters on the whole structure's behaviour depends on the impact energy, the structure's dimensions and the structure's boundary conditions. For example, the friction angle has limited importance as long as there is no large differential displacement. This influence increases with the block kinetic energy.

Reinforcement layers significantly improve the ability of an embankment to withstand the impact (ref. B2/B3 in Table 2). Such reinforcement layers, made of geogrid or geotextile, spread the impact load along the embankment axis (Peila et al., 2007). Nevertheless, such a beneficial effect implies a mechanical continuity of the geotextile layers, along the longitudinal axis of the RPE, requiring bonds or overlapping between two layers, while it's rarely the case.

The localized deformation of the embankment may result in burn-up of the reinforcement layer as well as in a tension along the longitudinal axis of the embankment. This differs from the static case accounting for gravity loads, where the reinforcement layer is loaded along the transverse axis of the embankment direction (Peila et al., 2002; Brandl and Blovsky, 2004). The impact load is thus distributed to soil masses at a distance on both sides of the impacted area. In the impact vicinity, the resulting confining effect by the layer increases the penetration resistance of the embankment. Moreover, if reinforcement also concerns downhill face of the RPE, the layer restrains the displacement of this face and thus increases the ability to withstand

the impact (Blovsky, 2002, 2004) (Figure 8). The negative counterpart is that horizontal planar reinforcement layers may offer a preferential plane for shear rupture (Figure 21).

Last, but not least, the impact response of the embankment strongly depends on the impact height: the closer the impact to the crest, the higher the penetration, with detrimental effects on the structure stability (Breugnot et al., 2015). Even if not addressed in detail, the impact inclination is thought to have a significant influence: the penetration is higher in case of a downward inclination according to Murashev et al. (2013) and higher for impact trajectories more or less perpendicular to the face (Kister, 2015).
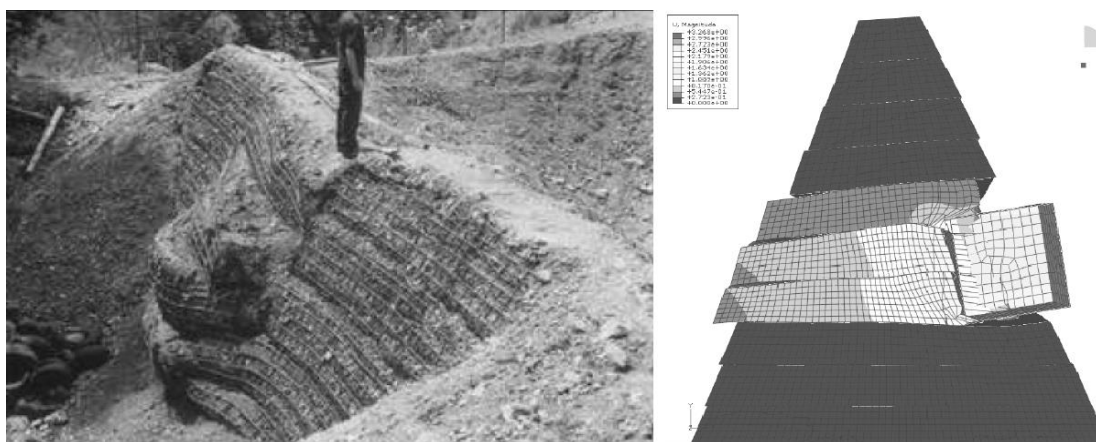

Figure 21 Reinforcement layers offer a preferential plane for shear rupture (Ronco et al., 2009).

3.3. Current design methods

In spite of their important protective role, the design of embankments is generally based on simplistic approaches. Also, contrary to rockfall protection galleries (or rock-sheds), there are neither recommendations nor guidelines concerning their design in any of the countries concerned, except the recent Austrian standard (ONR, 2013). Even if in some cases, specific and rather complex studies have been conducted (Lepert and Corté, 1988; Brandl and Blovsky, 2004; Lorentz et al., 2010), the vast majority of existing structures have been designed with basic approaches, considering dynamics only to a minor extent.

3.3.1. Typology of existing methods

The approaches in use today differ in their level of complexity and their ability to account for the dynamics. Existing structures have been designed considering different approaches (adapted from Lambert and Bourrier, 2013):

- Type 1: based on its mass, the embankment is assumed to be able to stop the block and withstand the impact. The structure is just designed with respect to gravity loads.

- Type 2: penetration criteria-based approaches estimate the penetration of the block in the embankment, which is multiplied by a factor of 2 to 3 to obtain the minimum embankment

thickness (Brunet et al., 2009). This is based on a criterion of post-impact stability of the deformed structure (Ronco et al., 2009).

- Type 3: pseudo-static approaches consider a load that is statically equivalent to the dynamic impact load for designing the embankment (Jaecklin, 2006; Kister and Fontana, 2011). A safety factor may be considered, expressing the uncertainties associated with the hypothesis of a statically equivalent loading (Brandl and Adam, 2000). The structure's static stability is checked based on classical methods devoted to embankment stability while considering this load in combination with gravity loads.

- Type 4: energy approaches assess the ability of the embankment in withstanding the impact based on analytical estimations of the energy dissipated within the embankment. In this purpose, the impact can either be described in terms of block incident kinetic energy or impact force. Energy dissipation is computed considering an Impact Disturbed Zone (IDZ). The IDZ is the volume of the RPE exposed to severe loading resulting in large displacements, strains, and changes in the mechanical characteristics. The first dissipative mechanism accounted for is friction along shear planes assuming that the IDZ moves as a rigid body (Tissières, 1999; Brandl and Adam, 2000; Kister and Fontana, 2011; Kister, 2015). In reinforced structures, the IDZ is often delimited by the reinforcement layers offering a preferential shear rupture plane (Ronco et al., 2009; Carotti et al., 2000). Energy dissipation through soil compaction can also be considered either by analytical approaches (Jarrin, 2001) or by considering of ratio of compaction energy dissipation (Ronco et al., 2009; Kister, 2015). The design consists in assessing that the structure deformation required to dissipate the block's kinetic energy is consistent with the embankment dimensions. For this purpose, the uphill deformation due to the block penetration may be deduced from the impact force (Ronco et al., 2009).

- Type 5: numerical modelling approaches, based on specific numerical tools for modelling the impact and evaluate the deformation of the embankment, using either finite difference or finite elements methods (FDM, FEM) or discrete element methods (DEM) (e.g. Peila et al., 2007; Lorentz et al., 2010; Jarrin and Meignan, 2010; Murashev, 2013; Breugnot et al., 2015).

Types 2–4 generally involve determining the block penetration or the impact force. Different equations have been proposed for determining either the one or the other with respect to rockfall related applications (Table 4). Details concerning these equations are provided in the next sections.

Types 5 approaches being less accessible to design engineers in general, as requiring specific skills and backgrounds, these will not be detailed in the following. Priority is given to analytical methods more commonly used, which are much more accessible and rapid to use.

The proposed classification is similar to that proposed by Kister (2015), considering design approaches 2 to 4.

3.3.2. Block penetration estimation

The penetration of a block into the embankment has been estimated using different equations, depending on the author as illustrated in Table 4. These are detailed in the following, together with equations that are relevant in the field of rockfall. The original expressions have been modified considering a same system of symbols and using SI units as defined in Table 5.

These methods and their limitations will be discussed in section 3.3.4.

Table 4 Methods for estimating the block penetration and impact force, explicitly used for RPE design purpose

	Method proposed by	Referred to in
Penetration	Kar (1978)	Paronuzzi (1989), Carotti et al. (2004), Maccaferri (2009), and Frenez et al. (2014). Specifically accounting for reinforcement layers in Cargnel and Nössing (2004);
	Calvetti and di Prisco (2007)	Brunet et al. (2009)
	Grimod and Giacchetti (2013)	Willye (2014)
Force	Mayne and Jones (1983)	Peila et al. (2007)
	Montani (1998)	Jaecklin (2006)
	Labiouse et al. (1996)	Peila et al. (2007), Ronco et al. (2009), Frenez et al. (2014)
	FEDRO (2008)	Kister and Fontana (2011)

Table 5 Symbols used in sections 3.3.2 and 3.3.3

Symbol	Unit	Definition
E	kPa	Young's modulus of the impacted material
E_s	kPa	Young's modulus of the projectile
F_i	N (unless specified)	Impact force
F_i^*	N (unless specified)	Characteristic value of the impact force (generally the maximum impact force, unless specified)
g	m/s²	Gravity
G_{dyn*}	kPa	Shear modulus of the impacted material
H_c	m	Projectile free falling height
m	kg	Mass of the projectile
M_E	kPa	Impacted material static elastic modulus (Swiss standard)
N	-	coefficient depending on the shape of the projectile (nose factor)
N_γ	-	Soil bearing capacity factor
p	m	Block penetration
r	m	Radius of the projectile (sphere or equivalent sphere)

t	m	Soil layer thickness
v	m/s	Projectile velocity before impact
ϕ	Rad	Friction angle of the impacted material
γ	kN/m^3	Soil unit weight
σ_d	kPa	unconfined compressive strength of the impacted material
ν	-	Poisson coefficient of the impacted material

Kar (1978) evaluated the penetration depth of bombs and missiles on soil protection shelter structures, based on real scale experiments. Kar (1978) proposed determining the penetration from:

$$p = \frac{4.06 \cdot 10^5}{\sqrt{\sigma_d}} \cdot N \cdot \left(v \cdot \frac{E}{Es} \right)^{1.25} \cdot \frac{m}{r^{2.31}} \tag{1}$$

Calvetti and di Prisco (2007) proposed the chart in Figure 22 for estimating the penetration depending on the block falling height and radius. This chart was obtained from numerical simulations using the BIMPAM model, calibrated using results of impacts of a 850-kg boulder on granular layers with 1 to 2 m in thickness.

It is here proposed that this chart is conveniently captured by:

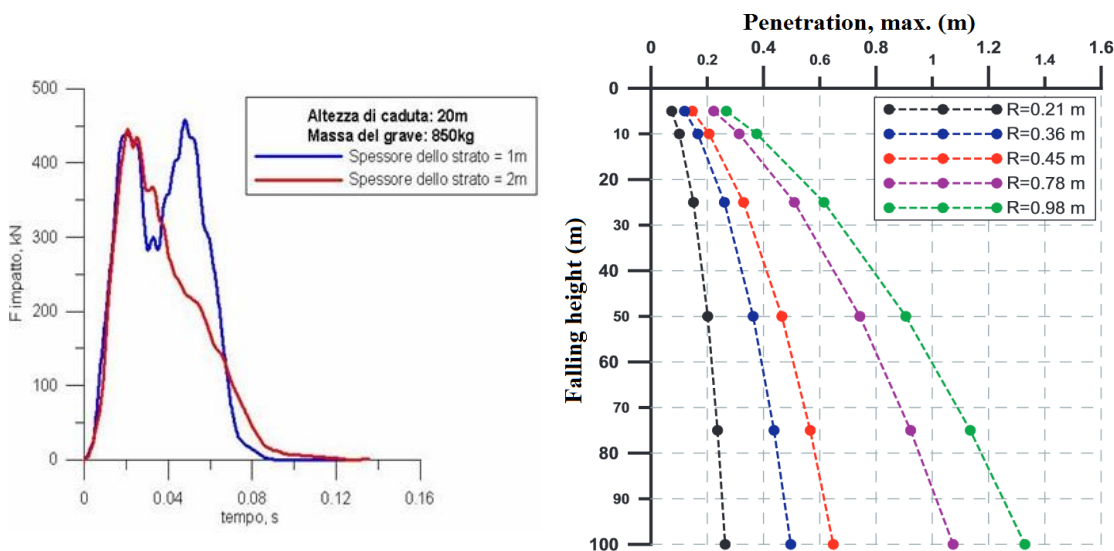$$p = 0.027 \cdot r \cdot v + 0.24 \tag{2}$$

Figure 22 Based on impact experiments with an accelerometer-equipped sphere (left) Calvetti and di Prisco (2007) proposed a chart fort estimating the block penetration

Pichler et al. (2005) considered formulae developed for non-deformable ogive-nose impactors penetrating concrete and soil targets, and proposed by Li and Chen (2003):

$$p = 2 \cdot r \cdot \sqrt{\frac{1 + k\pi/4N'}{(1 + I/N')} \cdot \frac{4k}{\pi} \cdot I} \,, \qquad when \ \ p \leq 2 \cdot r \cdot k \qquad (3)$$

$$p = \frac{4 \cdot r}{\pi} \cdot N' \cdot \ln \left[\frac{1 + I/N'}{(1 + k\pi/4N')} \right] + k \,, \qquad when \ \ p \succ 2 \cdot r \cdot k \qquad (4)$$

In these expressions, I is related to the impact intensity, N' depends on the mass, shape and radius of the projectile, and type and mass density of the impacted material, and k is the dimensionless depth of a surface crater.

I is given by:

$$I = \frac{m \cdot v^2}{8 \cdot R \cdot r^3}$$

Where R is a strength-like indentation resistance of the impacted materials.

In the experiments conducted by Pichler et al. (2005) with cubic boulders dropped on coarse gravel, R was found to vary between 8.13 and 10.98 MPa and N' equal to 2.385. More detailed information concerning the calculation of I and N' can be found in Pichler et al. (2005).

The parameter k strongly depends on the projectile tip shape, according to Figure 23. If the tip is flat, k should be set to 0.707*(2r), according to the theory of Prandl. If the tip of the projectile is curved or cone-shaped, then it will penetrate the target, which is assumed as half-space. In these cases, k may be defined as k = 0.707+H/(2r) where H is the height of the tip. Consequently, for a projectile with a hemispherical tip k = 1.207.
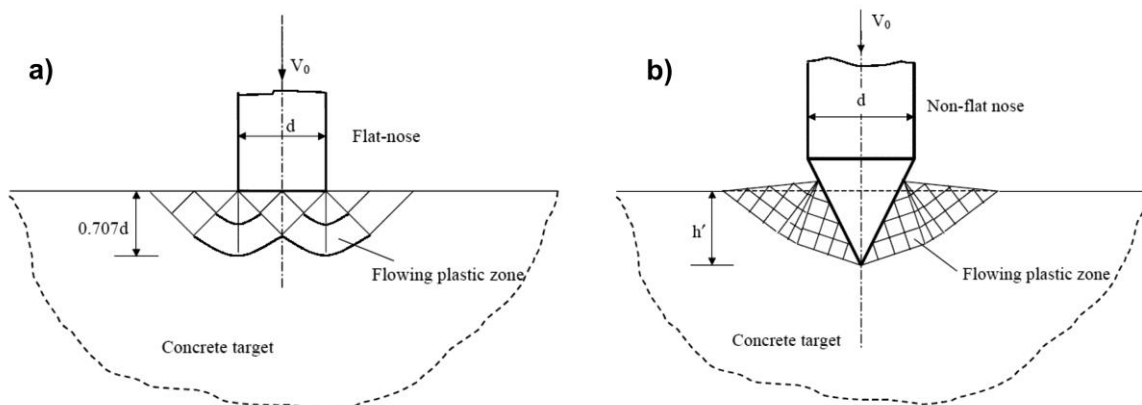

Figure 23 Slip line field of concrete crater created by a) a flat-nose projectile, b) by a projectile with arbitrary nose (Li and Chen, 2003).

Based on the work conducted at the University of Torino, Grimod and Giacchetti (2013) proposed to determine the penetration with:

$$p = p_c \cdot \frac{1}{2} \cdot m \cdot v^2 \cdot \frac{k}{\pi \cdot r^2} \tag{5}$$

Where p_c is the ratio of the block kinetic energy that is dissipated by plastification in the embankment (typically 0.85, see Ronco et al. 2009), k is a coefficient depending on the reinforcement material and the type and compaction level of the soil. This estimate is considered by Willye (2014) while also accounting for a factor depending on the block shape.

Based on a similar approach as that used for shallow foundations design, Wang and Cavers (2008) proposed:

$$p = \left(\frac{m \cdot v^2}{1.067 \cdot \gamma \cdot N_\gamma} \right)^{0.33} \tag{6}$$

Finally, if the impact force is known, based for example on the estimation methods presented in the next section, the block penetration, can also be computed as:

$$p = \frac{m \cdot v^2}{F_i} \tag{7}$$

This relation is obtained from the work done by the force acting on the embankment over the whole impact duration, considering that the block velocity is then 0. This work equals the translational kinetic energy of the block before impact, given by:

$$KE_{trans} = \frac{1}{2} \cdot m \cdot v^2 \qquad W = \int F_i \cdot dx = F_{medium} \cdot p$$

If the maximum is considered as the characteristic impact force value, F_i^*, and assuming that the maximum impact force is twice the medium force, this yield to:

$$\frac{1}{2} \cdot m \cdot v^2 = \frac{1}{2} \cdot F_i^* \cdot p$$

and finally to equation (7).

Equation 7 has been used by Carotti et al. (2004), Peila et al. (2007), FEDRO (2008) and Ronco et al. (2009) among others.

Other existing formulas developed with the aim of estimating the penetration of rigid bodies (projectile…) in soil are not detailed here as these are not referred to in rockfall engineering related documents (see for example a list in Montani, 1998).

3.3.3. Impact force estimation

As a preliminary comment, it must be pointed out, that the definition of a static force that is equivalent to a dynamic loading, F_i^*, is not straightforward. Most often, the maximum impact force is considered as the characteristic value to be used for this purpose, but this may be an asymptotic value, due to the shape of the impact force curve with time revealing that the maximum correspond to a very short duration peak by comparison with the whole impact duration (Lambert et al., 2014).

Different expressions have been proposed for determining the impact force of a rigid body onto soil, either issued from ground compacting technique developments or from research in the field of rockfall. The expressions presented in the following have been explicitly used for RPE design purpose (Table 4). Again, the original expressions have been modified considering a same system of symbols and using SI units, as defined in Table 5. These methods and their limitations will be discussed in section 3.3.4.

Based on ground compaction tests, Mayne and Jones (1983) proposed:

$$F_i^*\left[kN\right] = \sqrt{\frac{32 \cdot H_c \cdot G_{dyn}^* \cdot r \cdot m \cdot g}{\pi^2 \cdot (1-v)}} \tag{8}$$

Labiouse et al. (1996), proposed to use an expression derived from the elastic collision theory (Hertz):

$$F_i^*\left[kN\right] = 1.765 \cdot r^{0.2} \cdot M_E^{0.4} \cdot \left(m \cdot H_c \cdot \frac{g}{10^3} \right)^{0.6} \tag{9}$$

Even though this expression is directly derived from the Hertz theory, a rather good agreement was obtained with the impact results (Labiouse et al., 1996; Montani, S., 1998). These tests concerned a granular layer 0.35 to 0.5m in thickness, resting on a concrete structure and impacted by boulders with energies up to 100 kJ, without rotation.

Based on the same set of experiments, Montani (1998) proposed the following equation for computing the impact force:

$$F_i^*\left[kN\right] = 1.35 \cdot \exp\left(\frac{r}{3 \cdot t}\right) \cdot r^{0.2} \cdot M_E^{0.4} \cdot (\tan\phi)^{0.2} \cdot \left(m \cdot H_c \cdot \frac{g}{10^3} \right)^{0.6} \tag{10}$$

This relation was derived from the Hertz theory and was checked to be consistent with results of the impact experiments in the case of a granular layer resting on a slab.

The Swiss guideline concerning rockfall protection galleries (FEDRO, 2008) considered the previously mentioned work for proposing that the impact force on the cushion layer covering the galleries is obtained by:

$$F_i^* [kN] = 2.8 \cdot t^{-0.5} \cdot r^{0.7} \cdot M_E^{0.4} \cdot \tan\phi \cdot \left(\frac{m \cdot v^2}{2} \cdot \frac{1}{10^3} \right)^{0.6} \tag{11}$$

The Japanese Rockfall Protection Handbook (JRA, 2000; see also Yoshida et al., 2007), considering the classical model of the elastic collision of two spheres, proposed a formula for an impact of a block onto a cushion layer covering a shed:

$$F_i^* [kN] = 2.108 \cdot \left(\frac{m \cdot g}{10^3} \right)^{0.66} \cdot \lambda^{0.4} \cdot H_c^{0.6} \cdot \left(\frac{t}{2 \cdot r} \right)^{-0.58} \tag{12}$$

According to the authors, the parameter λ typically ranges from 1000 kPa for sand, up to 3000 kPa for compacted fill. Even if introduced by the authors as such, this parameter should not be considered as the Lame's parameter used in the theory of elastic waves.

Plassiard and Donzé (2009) presented a formula for the equivalent static force deduced from numerical simulations using the Distinct Element Method (DEM). The model parameters were calibrated using the results of the experiments conducted by Pichler et al. (2005). For the impact of a sphere on an embankment with a symmetric cross section they found that the equivalent static force is only a function of the kinetic energy of the block:

$$F_i^* = 225 \cdot \left(\frac{m \cdot v^2}{2} \right)^{0.66} \tag{13}$$

Ploner et al. (2005) considered Newton's second law, which can be expressed as:

$$m \cdot \Delta v = \int_{\Delta t} F_i dt$$

From the impact experiments presented in Montani et al. (1998), Ploner et al. (2005) considered an impact duration Δt of 50 ms. During this period, the block is stopped and, consequently, $\Delta v = v$. Finally, Ploner et al. (2005) considered that the impact force was constant during the impact, leading to:

$$F_i^* = \frac{m \cdot v}{\Delta t} \tag{14}$$

Ploner et al. (2005) used this force value for embankment design purpose. It is worth highlighting that the average is considered, and not the maximum impact force value.

On the contrary, Hofmann and Mölk (2012) considered the maximum value of the impact force, leading to the equivalent static force given by:

$$F_i^* = \frac{2 \cdot m \cdot v}{\Delta t} \tag{15}$$

But equation (15) is referred to be used just for checking the results received by:

$$F_i^* = \frac{v^2 \cdot m}{p} \tag{16}$$

The penetration depth p in equation (16) to estimate the equivalent static force will be taken out of the diagrams in Figure 32.

3.3.4.   Limitations in Types 2 - 4 approaches

The analytical methods mentioned in the previous sections and corresponding to the design approaches of types 2 to 4, provide design engineers with easy-to-use tools. Nevertheless, their relevancy is limited due to the uncertainty associated with each method, resulting from over-simplifications or shortcuts.

Estimation of the impact force and block penetration

For instance, the penetration is overestimated by up to a factor of 2 using the expression proposed by Kar (1978) whereas it is underestimated down to about 50% using the models proposed by Labiouse et al. (1996) and by Mayne and Jones (1983) (Oggeri et al., 2004; Carotti et al., 2004; Peila et al., 2007). Symmetrically, the opposite trends are observed when estimating the impact force. For a specific case, a ratio of 1:5 between the highest and the lowest impact force values may be obtained depending on the method considered (Kister and Fontana, 2011).

Figure 24 shows the equivalent static forces estimated from different methods in the case of a block with a diameter of 2.5 m and a velocity of 20 m/s impacting an unreinforced embankment with a crest width of 2 m (named b in this figure). The smallest value for the equivalent static force is given by the formula of Plassiard and Donzé (2009) for embankments with a symmetric cross section. On the opposite, the FEDRO formula results in the highest value when considering a layer 0.5 m in thickness (named t in this figure). In the end, the force varies in a ratio of 1 to 4 depending on the method.
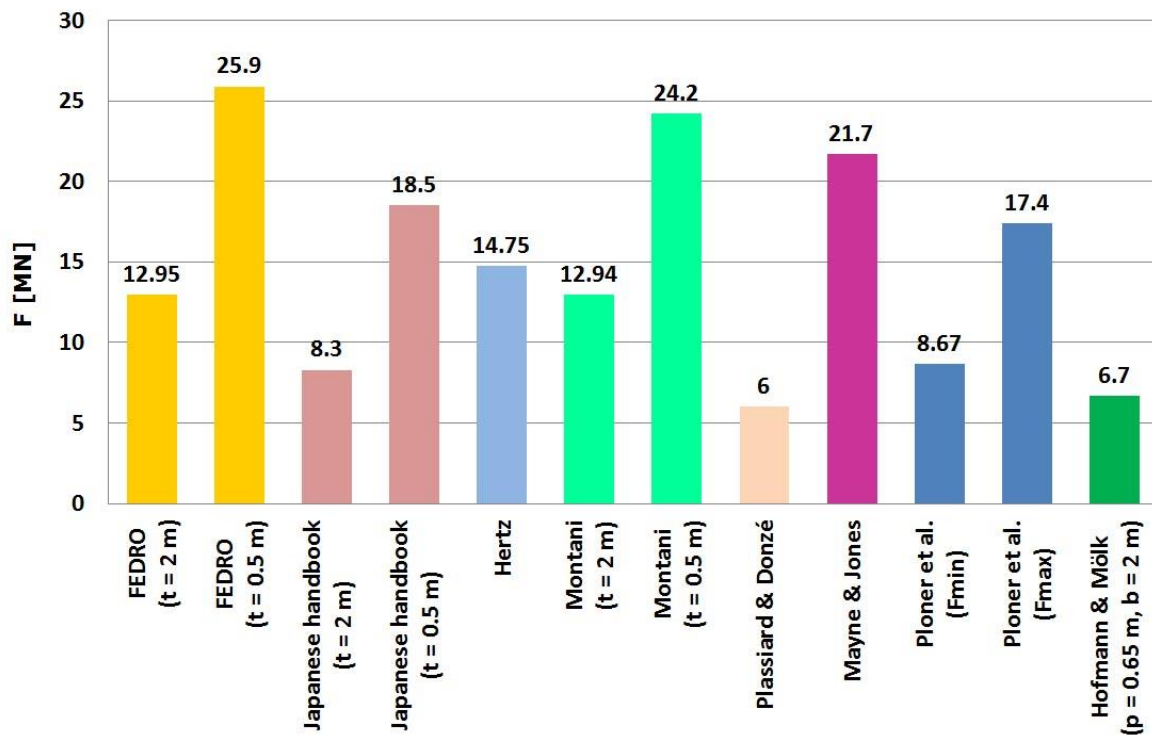
Figure 24 Equivalent static force estimated from different models (2.5 m block diameter and 20m/s initial block velocity) (Kister and Fontana, 2011, supplemented)

The main reason for these differences is that many of these methods were derived from experiments conducted in specific contexts that differ from the impact of a block on a RPE. Kar's model was developed for cohesive non-frictional soils impacted by ogive-nose projectiles at a minimum velocity of 300 m/s. Mayne and Jones's model was developed for heavy soil tamping, with a hammer having a flat tip. Labiouse's model was developed for granular strata, a 1-m maximum thickness, lying on a rigid support and exposed to impact by a spherical object amounting less than 100 kJ in energy.

Compared to the impact of a block on an embankment, these contexts differ in the projectile velocity and shape as well as the impacted structure's mechanical characteristics, dimensions and boundary conditions. An embankment is a free-standing finite volume structure, typically 3 to 7 meters in thickness in the impact direction. It is most often made of frictional non cohesive materials. It is exposed to the impact by blocks, more or less cubic or spherical in shape, with velocities in the range of 5-30 m/s, and energies from 1000 kJ to tens of MJ.

The difference in boundary conditions concerns equations 9 - 12, proposed by Labiouse et al. (1996), Montani (1998), FEDRO (2008) and JRA (2002), respectively. To a lesser extent, equations 3, 4 and 6, proposed by Pichler et al. (2005) and Wang and Cavers (2008), may also be concerned as based on experiments on a semi-infinite domain. Because some of these equations account for the impacted soil layer thickness (equations 10 - 12) their use for RPE

design purpose is tricky due to the difficulty in defining the thickness to consider (Kister, 2015).

The difference in loading conditions mainly concerns equations 1, 3 - 4 and 7. Some equations were derived from experiments conducted with ogive-nose projectiles with velocities up to 10 times that of rockfall, and without rotation. In Addition, most of these involved materials differing very much in their properties from soil, like for example concrete.

Equations 14 and 15 require assumptions concerning the impact duration (Δt). This impact duration depends on the construction material, in particular of the face (rip-rap vs. compacted soil for example). It also depends on the embankment width, as the impact by large blocks may induce a global RPE displacement conversely proportional to its width, resulting in longer impact duration for impacts close to the crest (Breugnot et al. 2015). Also, the shape of the block has a significant influence on the impact duration (Breugnot et al. 2015). This parameter may be rather variable with strong consequences on the force computed according to equations 14 or 15. For instance, according to Hofmann and Mölk (2012) Δt may vary in the interval 0.05 to 0.15 s for unreinforced embankments. For embankments reinforced with geogrids, Δt may vary in the interval 0.10 to 0.20 s (Figure 25).
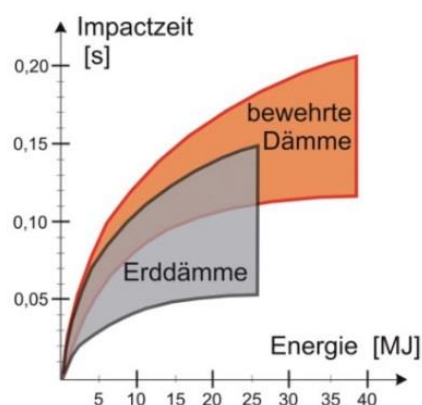

Figure 25 Impact duration estimated by Hofmann and Mölk (2012) and considered in ONORM (2013).

On the contrary, equations 5 and 13, proposed by Grimod and Giacchetti (2013) and Plassiard and Donzé (2009), are relative to embankments impacted by blocks. Nevertheless, in the former case the question of the extrapolation to other type and shape of structures rise. In the later, the proposed equation is based on numerical simulations and the same authors have shown it depends on other parameters too (Plassiard and Donzé, 2010).

It should be noted that the soil parameters considered in some of these equations are derived from static tests and concern the elastic response of soils: M_E, E and ν. The question of the validity of models intended to mimic high strain response of granular systems based on such parameters rise. Additional the parameter λ, which is used in the Japanese Rockfall Protection Handbook, does not agree with the definition of the Lamé parameter, which is used in the theory of elasticity and propagation of acoustic waves. A discussion on this is given in Kister

(2015). Mölk and Hofmann (2013) suggest that in general soil parameters are more favourable at dynamic loading than at static loading. On the other hand, for example, the shear modulus G decreases with increasing shear strain (**Erreur ! Source du renvoi introuvable.**).

Even if for specific contexts, the various authors found an agreement between experimental results and predicted ones, there is no real guarantee concerning the validity of the models, based on these parameters, when considering other materials or loading conditions (i.e. block size and velocity).
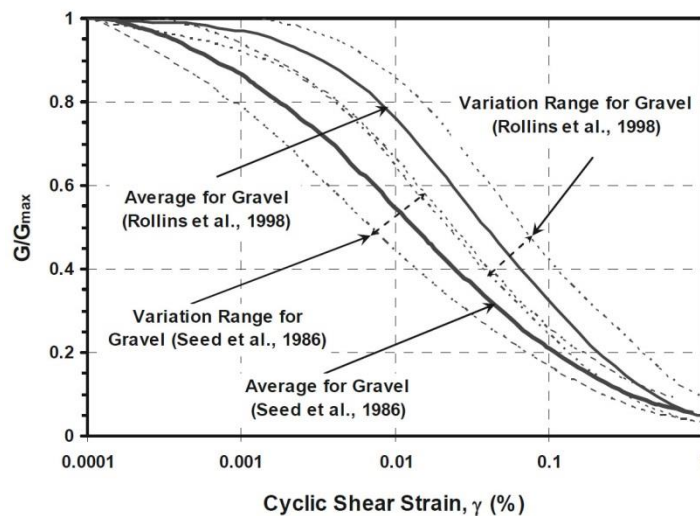

Figure 26 Typical G/Gmax ~ γ relationships for gravels (Liao et al., 2013).

In the same vein, the interaction between the soil and reinforcing geosynthetic, in terms of both interface friction and confining effect, has never been addressed to localized impact loading. The friction between these materials is modelled using friction angles and cohesion values derived from pull-out and shear tests with comparatively low deformation rates, whereas this interface has been clearly shown to govern embankment collapse (Peila et al., 2007; Ronco, 2009). Complementary investigations on the impact response of the different materials are therefore necessary. This will improve numerically based extrapolations to high-impact-energy events. The dynamic interaction between the geosynthetic and the soil should be investigated as a priority, focusing first on the friction and then on the confinement effect by the geosynthetic material in cases of localized impact.

The only equation introducing a parameter related to dynamics is equation 8, provided by Mayne and Jones (1983). They used a dynamic shear modulus G_{dyn}* instead of a static modulus of elasticity. But because the dynamic shear modulus is a function of the shear strain γ, they defined the value of G_{dyn}* as one-tenth of the dynamic shear modulus G_{max}, measured for small strains in seismic tests (**Erreur ! Source du renvoi introuvable.**). This relationship was primarily found by Hansbo (1977, 1978) for dynamic consolidation of soil and rockfill by falling weight.

Relevancy of the static equivalent load
Apart from the previous comments made on the analytical methods, the approach consisting in considering a statically equivalent load for modelling the impact force (Type 3) may not be fully appropriate.

The main reason is that this approach neglects some of the mechanisms at work during the impact, which governs the actual response of the whole structure, as depicted in section 3.2. In particular, this response depends on the stress transmitted with time within the structure, which in turn depends not only on the impact force, but also on other geometrical and mechanical parameters related to the embankment. It has been shown that for a given impact force the granular material characteristics may strongly affect the maximum value of the transmitted stress as well as its spatial distribution (Laue et al., 2008; Lambert et al., 2009; Heymann et al., 2010; Calvetti and di Prisco, 2011). The shape of the block has also been shown to have an influence on the impact force and on the transmitted stress (see the state of the art as described in Montani, 1998; Degago, 2007). And, this transmitted stress is a key factor in the RPE collapse, as suggested in section 3.2. The impact force is thus not only difficult to estimate, but is also partly inappropriate to account for what occurs within the embankment.

Relevancy of energy approaches
The analytical energy approaches (Type 4) are attractive in the sense they are based on phenomenological considerations. Nevertheless, their reliability depends on the quantification of the different energy dissipation terms: soil compaction first and then friction along shear planes. This implies defining a priori the IDZ volume and surfaces concerned by compaction and friction, respectively whereas these strongly depend on the loading conditions (impact energy and impact point location) and embankment material characteristics, which constitute the limitations of energy analytical approaches.

The first assumption concerning these methods is the definition of the IDZ. Tissières (1999) proposed a very simple model of the IDZ (Figure 27), defined by two vertical planes distant of the block diameter, and by a horizontal plane parallel to the foundation of the RPE. Hofmann and Mölk (2012) considered that the position with respect to the vertical axis of the horizontal plane delimiting the IDZ was defined by the block lower point (Figure 27). Based on an ultimate strength kinematic approach, Subrin et al. (2006) proposed to consider a basal plane with an inverse inclination (Figure 28).
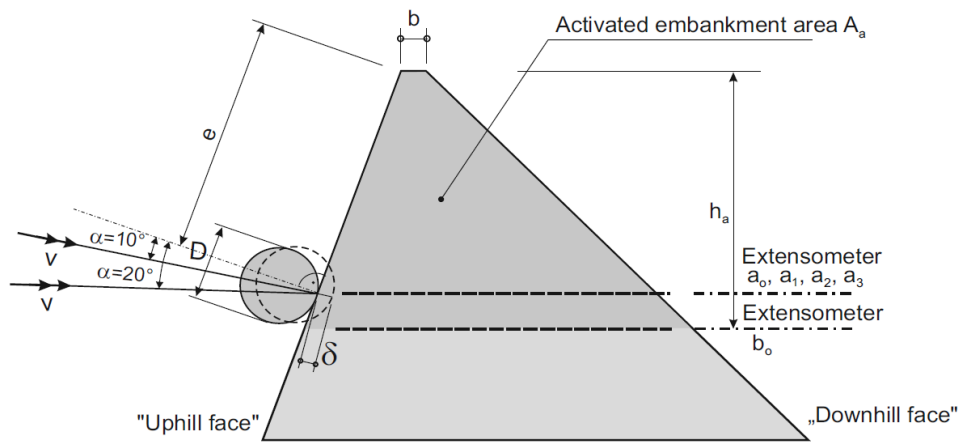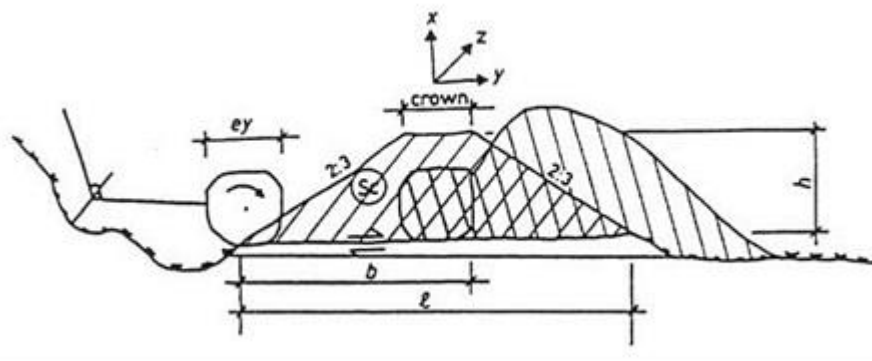
Figure 27 Model of the impact disturbed zone (IDZ) considered by Tissières (1999) (top) and by Hofmann and Mölk (2012) (bottom).
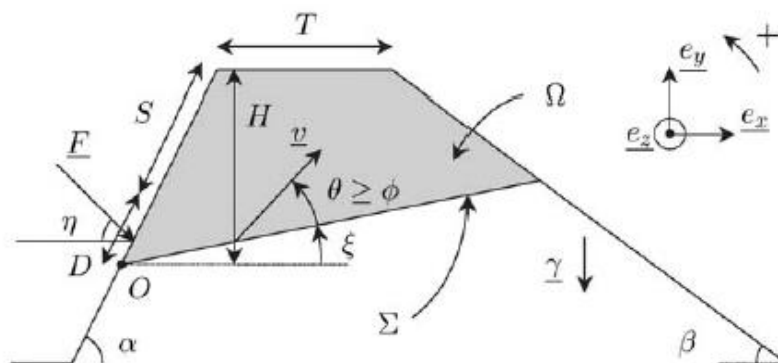

Figure 28 IDZ considered by Subrin et al. (2006).

In order to account for the block incident inclination, some authors have proposed to tilt the basal face of the IDZ (Kälin, 2006; Frenez et al., 2014; Kister and Fontana, 2011) (Figure 29). Kälin (2006) justified this choice based on the experiments conducted by the University of Torino on an unreinforced RPE (ref. B3 in Table 3) before using this IDZ for the design of the embankments of Wilerwald.
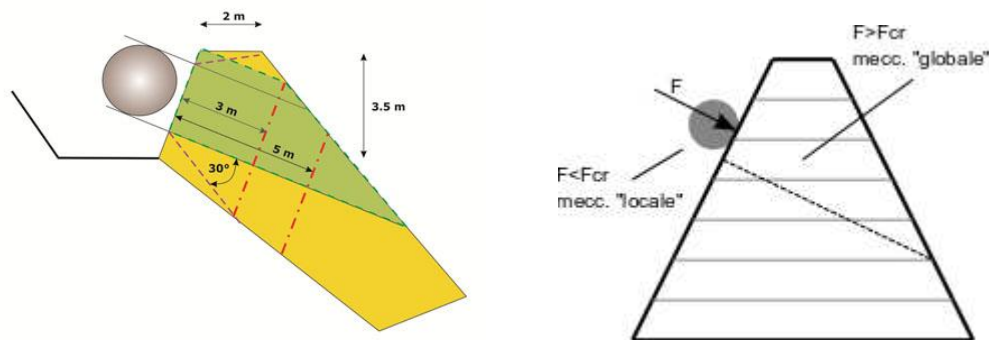

Figure 29 IDZ considered by Kister and Fontana (2011) (left) and Frenez et al. (2014) (right).
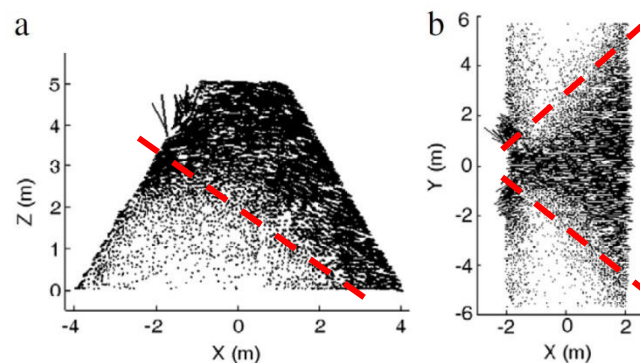

Figure 30 Displacement within the RPE during the impact. Results of DEM simulations a) by cross section, b) horizontal slice. (Plassiard and Donzé, 2009).

The idea of a tilted basal face of the IDZ seems to be underpinned by results of numerical simulations by Plassiard and Donzé (2009, 2010). Their results show relatively large displacements inside the embankment body above an inclined plane (Figure 30 a).

The IDZ is also delimited by two lateral planes. The simplest approach consists in considering two vertical and parallel planes, distant of the block diameter (Tissières et al., 1999, Kälin, 2006; Frenez et al. 2014). It is in contradiction with results presented in Figure 30 b showing that the IDZ forms a cone. This was observed in small scale experiments (Hofmann and Mölk, 2012; Blovsky, 2002, 2004) as well as in real scale experiments (Peila et al., 2002). Moreover, the dimension of the IDZ in the longitudinal axis has been shown to be higher than 5 times the block diameter for different small scale structure types (Mölk and Hofmann, 2013).

Last, the quasi-2D and 3-D experiments conducted by Kister (2015) suggested that the IDZ shape is much more complex than that proposed by the different models.

In the end, the definition of the IDZ appears highly questionable, in terms of geometry, while it is of paramount importance for computing the dissipated energy with these methods.

3.3.5. Limitations in Types 5 approaches

Existing numerical models have mainly been developed in research contexts. Some were used for developing design charts, designing specific structures, or to back analyse natural impacts (e.g. Ronco et al., 2010, Lorentz et al., 2010; Jarrin and Meignan, 2010; Peila, 2011; Murashev et al., 2013).

Even if, at first glance, models developed based on commercially available software seems easy to use, satisfactorily modelling the impact response of RPE requires highly specific skills. This in particular concerns not only the constitutive laws and mechanical characteristics to consider but also a comprehensive knowledge of the different numerical methods and theirs limits. For this reason, numerical tools are out of reach of most of the companies concerned by the design of RPEs. Also, the computation time is very long for some of the existing numerical models (Breugnot et al., 2015).

Besides, as for any numerical model an experimental data based calibration is required for guarantying the validity of the simulation results. Most often, the model parameters are calibrated based on static tests, such as triaxial tests. Some models have been validated by comparison with impact tests, on soil layers or RPEs. But due to the limited number of real scale experiments, and consequently the limited variety in structure type concerned, this validation cannot be conducted for any type of RPE, in terms of geometrical and mechanical characteristics, as well as impact conditions. Simulations out of the cases considered in the experiments should be considered as extrapolation, with possible consequence on the results relevancy. This holds for any type of modelling approach (FEM, FDM or DEM).

Other limitations more specific to the considered modelling approach may raise. For example, the DEM seems to be an ideal tool for modelling the RPE response to impact as it represents it as a collection of discrete elements and it is based on Newton's law of motion. But, in order to keep the computation time reasonable, each element is chosen much larger than the grain constituting the debris used for a real embankment's construction material (Figure 31). The difficulty is then to define the "micro-parameters" governing the interaction between these large particles so that the macro-response of the RPE represents an approximation of sufficient accuracy (see for example Breugnot et al., 2015 for a detailed description). This calibration may be based on triaxial tests results, complemented with free falling tests results, as for example in Plassiard (2007). In those back analysis the "micro-parameters" had to be varied in such a way that measured and calculated data fit together. But the question of the comparability of, for example, a slow-motion triaxial test and a high-dynamic impact scenario remains.

Figure 31 DEM model of embankment and block, both made of "glued" spheres (Plassiard and Donzé, 2010)

3.4. Applications of the Eurocodes

From a practical standpoint, the design of rockfall protection embankments challenges geotechnical engineers with the principles of currently used methods such as the Eurocodes.

Passive rockfall protection structures are not within the scope of specific Eurocodes and should be considered special structures. Moreover, the impact load should not be calculated as an accidental action according to EN 1991-1-7 (CEN, 2007), as the expressions given were developed for very different impacts and may lead to asymptotic values. Application of the Eurocodes principles requires accounting for the particular purpose of this type of structure. For example, Durville et al. (2010) have proposed a two-step procedure evaluating first the ability of the structure to intercept a block and second its post-impact residual characteristics. An ultimate limit state (ULS) verification is conducted considering the impact as an accidental situation and a block of a given mass, corresponding to a given scenario, and of maximum energy. The aim is to ensure that this block is stopped, even if the RPE collapses. Then a serviceability limit state verification is conducted to assess the post-impact embankment characteristics and considering an impact by the same block with a medium energy. This application of the Eurocodes is subjective and others could be considered.

Even if the principles of the Eurocodes may be adapted to the case of RPE, questions concerning the parameters defining the loadings may rise. The embankment response depends on both the energy of the block before impact and on the impact location. A low-energy event on the top of the structure may be more detrimental than a high-energy impact at its toe (Bertrand et al., 2010). Therefore, various combinations of these two variables should be considered, using their respective detailed statistical distributions. Moreover, the impact loading may be considered either accidental or variable, which influences the safety coefficients used for the design.

A straightforward application of the Eurocodes for the load case impact therefore does not appear meaningful. The engineer must manage the wide range of interpretation of these standards. The means to adopt the Eurocode principles, the definition of situations as well as the determination of the safety factors clearly remain the responsibility of the design engineer.

This has been briefly addressed in Grimod and Giachetti (2013), Grimod and Segor (2014) for designing existing structures. Ronco et al. (2009) also made reference to the Eurocodes for defining safety factors to be applied for the design block energy and passing height.

3.5. Italian recommendations

The Italian standard on the definitive and executive design of rockfall protection measures gives some recommendations for the input data for designing an RPE (Uni, 2012). No recommendation is given for the design properly speaking (i.e. how to use the input data for verifying the structure response). It is nevertheless indicated that the block penetration should be compared with the RPE width.

The design correspond to the case of a given single block volume in a given release area. The design of the RPE relies on the passing height and kinetic energy distributions of this block at the RPE location as obtained form trajectory simulations.

The impact point on the RPE is determined as the 95-% percentile of the design block passing heights distribution.

For this impact point, the design block velocity is the 95-% percentile of the velocity distribution, multiplied by a safety coefficient related to the trajectory simulation results quality. This coefficient varies between 1.04 and 1.21, depending on both the resolution of the digital elevation model and the way the restitution coefficients were determined.

The design block mass is the mass of the block estimated by geological survey multiplied by a safety coefficient depending on the method used to determine the volume (1.02 to 1.1).

The design kinetic energy is obtained from the design block velocity and design block mass. In case of human threat, this energy can be multiplied by a safety coefficient in the 1-1.2 range depending on the consequences in case of structure failure.

The Italian standard recommends that all the blocks from a given release scenario are stopped, accounting for the variety of block trajectories and rotational velocities in the RPE vicinity.

This standard is mentioned by Grimod and Segor (2014) for the design of the RPE built in Cogne (Italy). For this project, the structure was designed at the serviceability limit state in order to keep the deformation minimum after successive impacts, and thus reducing maintenance costs.

This standard provides a pragmatic framework for designing the RPE, mainly concerning the use of trajectory simulation results. It is worth highlighting that coefficients when cumulated range between 1.06 and 1.6, approximately, with huge consequences on the RPE cost and feasibility. Nevertheless, the maximum value may be reduced down to 1.3 if more precise data

are used for block mass estimation and propagation simulations. The main limitation in this standard is that no indication is given for the RPE design with respect to the block impact.

3.6. Austrian recommendations

The aim of this section is to briefly introduce the Austrian RPE structural design recommendations (ONR, 2013). This standard is based on the experiments conducted by Hofmann and Mölk (2012).

It explicitly refers to the Eurocodes (CEN, 2004). The impact by the rockfall is considered as an exceptional design situation, and the design addresses the ultimate limit state only.

The design block volume is established based on the block volume distribution and depends on the event frequency: percentile values of 95 to 98% of the volume distribution are considered from seldom to very high frequency events.

The design follows a type-3 approach. The static equivalent force is calculated from the impact energy, by estimating the block penetration in the structure and the impact duration.

The design considers a so-called dimensionless impact energy E^*:

$$E^* = \frac{m \cdot v^2}{2 \cdot \left(\rho \cdot g \cdot A_a \cdot D \cdot h_a\right)} \qquad (17)$$

Where m [kg] and v [m/s] are the mass and velocity of the block, ρ represents the soil density [kg/m³], g the gravity acceleration [m/s²], A_a the activated area [m^2], D the block diameter [m] and h_a the activated height of the IDZ [m] (see Figure 27).

The velocity considered corresponds to the 99-% percentile of the velocity distribution obtained conducting trajectory simulations with the design block.

The activated area is defined according to the principle defined in Figure 27, bottom. The activated height depends on the block passing height as defined in section 2.2 and on the block radius. The activated area is calculated as:

$$A_a = \frac{(b + c)}{2} \cdot h_a \qquad (18)$$

Where b and c are the crest width [m] and the width of the structure at the lower block point height [m], respectively. Replacing A_a in Equation (17) by Equation (18) shows very clearly that the height h_a has been taken into account twice, but the third dimension was not taken into account in this formulation of a dimensionless impact energy E^*.

With the calculated value of E*, the penetration depth δ is determined according to the chart presented in Figure 32.
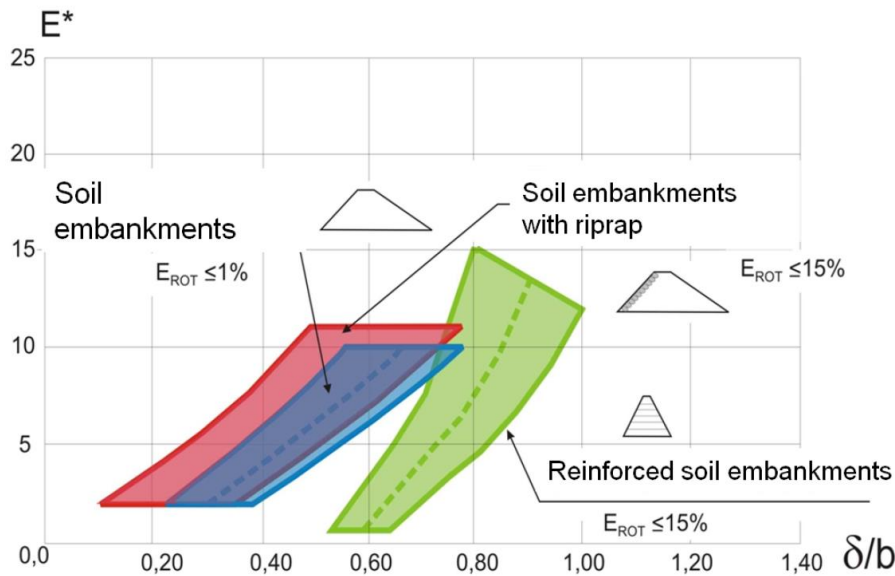

Figure 32 For a given embankment geometry and type, this chart may be used to estimate the block penetration δ for a given crest width b, and the dimensionless impact energy E according to Hofmann and Mölk (2013)*

The design equivalent static force is estimated using the formula:

$$F_d = \frac{v^2 \cdot m}{\delta} \cdot \gamma_{E,kin} \qquad (19)$$

Where:
- $\gamma_{E,kin}$ is a safety coefficient (1.0 to 1.15) depending on the consequence class,
- δ is the penetration depth determined according to Figure 25.

The static equivalent force estimated using equation (19) is applied to the IDZ, in addition to gravity loads, for assessing the ultimate limit service state (ULS). In this purpose, the force is applied in the direction of the incident trajectory inclination.

The standard does not provide any indication on the width of the IDZ to consider. Mölk and Hofmann (2013) suggest considering width of 5 - 6 and 8 - 9 times the block diameter for unreinforced and reinforced embankments, respectively.

Apart from the comments made in section 3.3.4 and in previous paragraph, this design approach is debatable in the sense many discrepancies appears in the method (Kister, 2015). These concerns:

- Experiments were conducted with a steel sphere, with a higher unit mass than a rock, resulting in a higher penetration (so-called "bullet effect");

- E* doesn't accounts for the IDZ width (see Eq. 17 and Eq. 18);
- The force-time and velocity-time diagrams considered are not consistent one with each other. The former is based on an elastic model, with symmetric behaviour with time, while the latter is based on a plastic model.

This standard makes reference to the block rotational energy. It appears in the chart presented in Figure 32 with complements given in an annex and recommending that the maximum part of rotational energy to total kinetic energy should be less than:
- 1% for pure soil RPEs;
- 15% for RPEs with a rockery facing as well as for reinforced RPEs.
Nevertheless, there are no data supporting these limits and the value given for pure soil RPEs seems unrealistically low in practical.

It also has to be taken into account that the application of the ONR 24810:2013 may lead to large constructions as shown for an example in Figure 33.
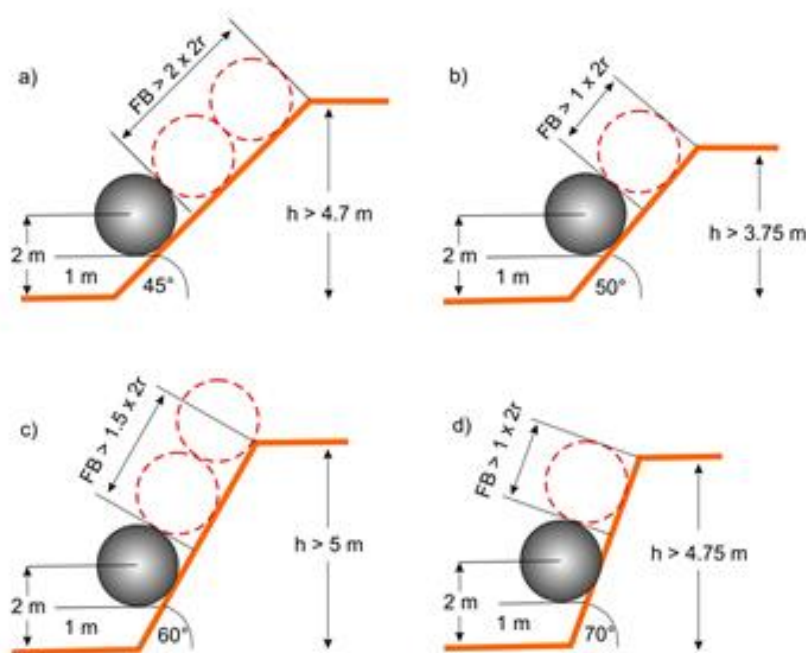

Figure 33 Visualization of the recommendations given in ONR 24810:2013 for the freeboard (see Table 2) for a block with diameter 2 m and passing height 2 m (measured to the mass centre)

4. Conclusion

RPE have been used for more than 50 years. Many research works have been conducted since the end of the 80's with the aim of improving their design, in particular with respect to the structure ability in withstanding the impact. Some of these research results have percolated down to engineering practices, either through national recommendations or design methods. In

particular, some recommendations have been published for defining the structure geometry (structure height and face inclination). Different engineering-oriented methods have been developed over the last two decades to predict the ability of RPE to withstand impacts.

Although embankment design with respect to both trajectory control and impact stability has been significantly improved, a number of limitations have been identified and should be kept in mind by design engineers.

The main limitations concerning the functional design of embankments stem from the rockfall simulation codes. In the design process, these codes are used to determine the rock passing heights and velocities respectively energies even though they are not calibrated for this purpose. Rockfall simulation codes are generally calibrated and/or validated by back analysis of previous rockfall events or rockfall experiments that are compared solely on the rocks' stopping distance. Trajectory analysis tools therefore provide relevant results for rock stopping distances: however their accuracy in estimating the rock kinematics is generally more limited. Most of the programs use simple physical models as the lumped mass model to calculate the trajectory and simple block geometry like a sphere or a cylinder for the description of the impact process with the topography. Additional, the coefficients of restitution defined only as a function of the block velocity before and after the impact, may not be able to describe the impact process with a sufficient accuracy (Kister et al, 2005, Bourrier et al., 2012). Modelling the mechanical interaction between the block and the embankment also has limitations. In particular, models for the interaction between the block and the embankment as well as with the surfaces in its vicinity lack of realism mainly due to limited knowledge on the actual impact response of the materials concerned. In addition, 3D rockfall simulation codes are currently used and calibrated with a spatial resolution that does not satisfactorily model the embankment shape (Lambert et al., 2013). Consequently, the spatial resolution of the models does not allow one to obtain a good estimate of the residual risk.

In terms of guidelines with respect to the functional design of RPE, recommendations defining a global methodology for, in particular, the definition of the design scenarios and protection goals as well as the use of rockfall trajectory simulations tools and their results are needed. These recommendations should account for the variety and limitations of the currently used tools as well as for the uncertainties. It should provide indications on the way to characterize the residual risk, based on the design scenario considered. A first draft of such a recommendation was given by Rovina et al. (2011) and could be updated and complemented.

As for embankment design with respect to impact, satisfactorily accounting for the dynamics, requires taking into account the complexity of the mechanisms at work during the impact and estimating their amplitude with time, which depends on the impact energy, embankment material characteristics and dimensions. As a consequence, analytical models are not yet satisfactory for this purpose. They fail to give good estimates of impact forces, block penetration, and energy dissipation terms. Numerical models are costly but may be identified as relevant tools for the design of embankments, providing a validation based on real-scale experiments involving impact energies of similar amplitude. In a research process, these

methods could be used jointly with experiments to improve current analytical models for different loading cases.

It has to keep in mind that RPEs generally are designed for a special scenario. So such a protection structure will only be able to offer a protection up to a certain decided level. But for this level a protection goal has to be defined. As protection goal the FEDRO defines the frequency of fatalities per year to be less than 10^{-5}. The protection goal defined by FOEN is a frequency of fatalities per year to be less than 10^{-4} - 10^{-5} (BAFU, 2016). Events corresponding to scenarios no considered or outside of the protection goal must be accepted as possible residual risk.

The analysis of existing experiments as well as existing recommendations given in this part A of the research report showed that there is still a lack of information concerning the design of RPE. Nevertheless the construction of RPEs is still going on and as it will be shown in part B of the report the basics used for the design of a RPE differ significantly from place to place in Switzerland. So there is a need for recommendations corresponding to the best practice. These recommendations should include references to the following topics:

- definition of scenarios and protection goals,
- simulation,
- design of the RPE,
- consideration of uncertainties and
- how to manage residual risks.

But also cross references to existing recommendations and standards as for example BAFU (2016) have to be included.

References

- Agliardi, F., Crosta, G.B., 2003. High resolution three-dimensional numerical modelling of rockfalls. International Journal of Rock Mechanics and Mining Sciences 40, 455-471.
- Agliardi, F., Crosta, G.B., Frattini, P., 2009 Integrating rockfall risk assessment and countermeasure design by 3D modelling techniques. NHESS 9, 1059-1073/
- Aminata, D., Yashima, A., Sawada, K., Sung, E., 2009. New protection wall against rockfall using a ductile cast iron panel. Journal of natural disaster science 30 (1), 25-33.
- BAFU, 2016. Schutz vor Massenbewegungsgefahren - Vollzugshilfe für das Gefahrenmanagement von Rutschungen, Steinschlag und Hangmuren
- Bertrand, D., Lambert, S., Gotteland, P., Nicot, F., 2010. Les merlons à technologie cellulaire. In: Lambert S., Nicot F. (Eds), Géo-mécanique des instabilités rocheuses: du déclenchement à l'ouvrage. Hermès, Paris, 369-402. (in French).
- Blovsky, S., 2002. Bewehrungsmöglichkeiten mit Geokunststoffen, PhD thesis, TU Wien.
- Blovsky, S., 2004. Model tests on protective barriers against rockfall. 15th European Young Geotechnical Engineers Conference, Dublin, Ireland.
- Bourrier, F., Lambert, S., Heymann, A., Gotteland, P., Nicot, F., 2011. How multi-scale approaches can benefit cellular structure design. Canadian geotechnical journal 48, 1803-1816.
- Bourrier, F., Hungr, O., 2011. Rockfall dynamics: a critical review of collision and rebound models. In: Lambert, S., Nicot, F. (Eds), Rockfall engineering. John Wiley and Sons, New York, ISTE ltd, London, 175-210.
- Bourier, F., Berger, F., Tardif, P., Dorren, L., Hungr, O., 2012. Rockfall rebound: comparison of detailed field experiments and alternative modelling approaches. Earth Surface Processes and Landforms, vol. 37, n° 6, 656-665.
- Brandl, H., Adam, D., 2000. Special applications of geosynthetics in geotechnical engineering. Proceedings of the 2nd European Geosynthetics Conference and Exhibition- Eurogéo II, Bologna, Italy, 305-310.
- Brandl, H., Blovsky, S., 2004. Protective barriers against rockfall. Proceedings of the 3rd European geosynthetics conference-Eurogéo III, Munich, Germany, 95-100.
- Breugnot, A., Lambert, S., Villard, P., Gotteland, P., 2015. A discrete/continuous coupled approach for modeling impacts on cellular geostructures. Rock Mechanics and Rock Engineering, Doi: 10.1007/s00603-015-0886-8.
- Broccolato, M. and Segor, V. and Recalcati, P. and Salis, S., 2010. Two major geogrid reinforced rockfall barriers in northern Italy; Proc of 9th International Conference on Geosynthetics, 1765-1768.
- Brunet, G., Giacchetti, G., Bertolo, P., Peila, D., 2009. Protection from High Energy Rockfall Impacts Using Terramesh Embankment: design and Experiences. Proceedings of the 60th Highway Geology Symposium, Buffalo, New York, 107-124.
- Burroughs, D.K., Henson, H.H., Jiang, S.S., 1993. Full scale geotextile rock barrier wall testing, analysis and prediction. Proceedings of Geosynthetics '93, Vancouver, Canada, 959-970.
- Calvetti, F., di Prisco C., 2007. Linee guida per la progettazione di gallerie paramassi. Starrylink, Italy (in Italian), 184 pp.
- Calvetti, F., di Prisco C., 2011. A new design method for rockfall shelters covered by granular layers. In: Lambert, S., Nicot, F. (Eds), Rockfall engineering. John Wiley and Sons, New York, ISTE ltd, London, 343-373.
- Calvino, A., Dumont, P., Durville, J.-L., Dussauge, C., Effendiantz, L., Evrard, H., 2001. Parades contre les instabilités rocheuses. Guide technique, Collection environnement, Les risques naturels, LCPC, Paris, 143 pp. (in French).

- Cargnel, O., Nössing, L., 2004. Comportamento di opere passive interessate da scoscendimenti massivi. Proceedings of Convegno Bonifica di versanti rocciosi per la protezione del territorio, Trento, Italy, 419-434.
- Carotti, A., Peila, D., Castiglia, C., Rimoldi, P., 2000. Mathematical modelling of geogrid reinforced embankments subject to high energy rock impact. Proceedings of the 2nd European Geosynthetics Conference and Exhibition- Eurogeo II, Bologna, Italy, 305-310.
- Carotti, A., di Prisco, C., Vecchiotti, M., Recalcati, P., Rimoldi, P., 2004. Modeling of geogrid reinforced embankments for rockfall protection. Proceedings of the 3rd European Geosynthetics Conference, Munich, Germany, 675-680.
- CCC, 2013. Technical Guideline for Rockfall Protection Structures. Christchurch City Council
  ○ 1. Version 2 Final March 2013, 26 p.
- CEN, 2004. EN 1997-1, Eurocode 7: Geotechnical design - Part 1: General rules. European committee for standardisation, Brussels, 168 pp.
- CEN, 2007. EN 1991-1-7, Eurocode 1 - Actions on structures- Part 1-7: General actions - Accidental actions. European committee for standardisation, Brussels, 62 pp.
- Chau, K.T., Wong, R.H.C., Wu, J.J., 2002. Coefficient of restitution and rotational motions of rockfall impacts. Rock mechanics and mining science 39, 69-77.
- Clerici, A., Giuriani, E., Cambiaghi, D., Isceri, A., Vassena, G., Marchina, E. and Cominoli, L. 2013. Rockfall Full Scale Field Tests. Landslide Science and Practice, Springer Berlin Heidelberg. Eds Margottini, Canuti, Paolo and Sassa, 461-467.
- Corté, J., Lepert, P., Rochet, L., 1989. Design of a protective system against rock falls; example of RN 90 highway. Revue générale des routes et aérodromes 669, 114-117.
- Coulon, E., Bruhier, J., 2006. Les merlons renforcés de protection. Proceedings of Rencontres géosynthétiques 2006, Montpellier, France, 367-372 (in French).
- Degago, S.A., 2007. Impact tests on sand with numerical modeling, emphasizing on the shape of the falling object. Masters Thesis, NTNU, Trondheim, Norway, 140 pp.
- Descoeudres, F., 1997. Aspects géomécaniques des instabilités de falaises rocheuses et des chutes de blocs. Publications de la société suisse de mécanique des sols et des roches 135, 3-11.
- Durville, J.-L., Guillemin, P., Berthet-Rambaud, P., Subrin, D., 2010. Etat de l'art sur le dimensionnement des dispositifs de protection contre les chutes de blocs. Collection Études et recherches des LCPC - série Géotechnique et risques naturels, Paris, 84 pp.
- FEDRO, 2008. Directive 12006: Actions de chutes de pierres sur les galeries de protection. OFROU, Bern, Switzerland, 22 pp.
- Frenez, T., Vecchiotti M., Danzi A., 2014. Un nuovo approcio per la progettazione di rilevati paramassi in terra rinforzata – il progetto di Chizzola (Ala, Trento). XXV Convegno nazionale di geotecnica. 4-6 giugno, Baveno.
- Gerbert, S., Hespel, F., 1999. Geotextile's reinforced wall for natural risk protection works. Proceedings of Rencontres géosynthétiques, Bordeaux, France, 147-150.
- Grimod, A. and Giacchetti, G., 2013. Protection from High Energy Impacts Using Reinforced Soil Embankments: Design and Experiences. Landslide Science and Practice, Springer Berlin Heidelberg. Eds Margottini, Canuti, Paolo and Sassa, 189-196
- Grimod, A. and Segor, 2014. V. Reinforced soil rockfall embankment to absorb high energy impacts along the regional road SR 507 Aymavilles-Cogne, Aosta (Italy); Proc. of GeoRegina 2014 september 28-october 1
- Hansbo, S., 1977; Dynamic consolidation of rockfill, Proc. 9th International Conference on Soil Mechanics and Ground Engineering, Vol. 2, pp. 241 - 246, Tokyo.
- Hansbo, S., 1978. Dynamic consolidation of soil by a falling weight, Ground Engineering, Vol. 11, pp. 27 - 36
- Hara, T., Tsuji, A., Yashima, A., Sawada, K., Tatta, N., 2009. Dynamic interaction between pile and reinforced soil structure - Piled Geo-wall. Proceedings of the International

Symposium on Prediction and Simulation Methods for Geohazard Mitigation, Kyoto, Japan, 457-463.

- Hearn, G., Barrett, R.K., Henson, H.H., 1995. Development of effective rockfall barriers. Journal of transportation engineering 121 (7), 507-516.

- Hearn, G., Barrett, R.K., Henson, H.H., 1996. Testing and modelling of two rockfall barriers. Transportation research record 1504, 1-11

- Hennebert, P., Lambert, S., Fouillen, F., Charrasse, B., 2014. Assessing the environmental impact of shredded tires as embankment fill material. Canadian Geotechnical Journal. Vol. 51 (5), p. 469–478, Doi: 10.1139/cgj-2013-0194.

- Heymann, A., Lambert, S., Haza-Rozier, E., Vinceslas, G., Gotteland, P., 2010. An experimental comparison of real–scale rockfall protection sandwich structures. Proceedings of the 11th International Conference on Structures Under Shock and Impact, Tallinn, Estonia, 15-26.

- Hoek, E., 2007. Practical rock engineering. Available online: http://www.rocscience.com/.

- Hofmann, R., Mölk, M., 2012, Bemessungsvorschlag für Steinschlagschutzdämme. Geotechnik, Vol. 35, pp. 22-33.

- Hofmann, R., Vollmert, L., Mölk, M. 2013. Rockfall-protection embankments - design concept and construction details. 18th International conference on soil mechanics and geotechnical engineering, Paris, 2-6 September 2013,

- Jaecklin, F., 2006. Innovative design for repairing Gondo mudslide by 20m high geogrid wall. Proceedings of the 8th international conference on geosynthetics, Ozaka, Japan, 1223-1228.

- Jarrin, P. 2001. Trajectographie des blocks rocheux. Master thesis, ENSMP, Paris.

- Jarrin, J.P., Meignan, L., 2010. Geomechanical modelling of rockfall protection bunds submitted to a dynamic impact. Proceedings of Journées Nationales de Géotechnique et de Géologie de l'Ingénieur JNGG2010 - Grenoble 7-9 juillet 2010

- JRA, 2000. Japan Road Association: Japanese Rockfall Protection Handbook (in Japanese)

- Kälin, A., 2006. Steinschlagverbauung Wilerwald, Gurtnellen, Projektbasis, Bauprojekt, 07.09.2006.

- Kar, A.K., 1978. Projectile penetration into buried structures. Journal of Structural Division, ASCE 104 (1), 125-139.

- Kister, B., Heldner, C., Ettlin, A., 2005. Der Einsatz numerischer Berechnungsverfahren zur Simulation der Steinschlagproblematik, Luzerner Baukolloquium Geotechnik, 4. März 2

- Kister, B., Fontana, O., 2011. On the evaluation of rockfall parameters and the design of protection embankments – a case study. Proceedings of Interdisciplinary workshop on rockfall protection - Rocexs 2011, Innsbruck, Austria, 31-32.

- Kister, B., Horat, P., Berger, T., 2014. Quasi-2D-experiments visualization of impacts on embankments. Proceedings of Interdisciplinary workshop on rockfall protection - Rocexs 2014, Lecco, Italy,

- Kister, B., 2015. Development of basics for dimensioning rock fall protection embankments in experiment and theory (in German), research project FEDRO 2012/003, FEDRO report 1524.

- Labiouse, V., Descoeudres, F., Montani, S., 1996. Experimental study of rock sheds impacted by rock blocks. Structural Engineering International 3, 171-175.

- Labiouse, V., Heidenreich, B., Desvarreux, P., Viktorovicth, M., Guillemin, P., 2001. Etudes trajectographiques, Prévention des mouvements de versants et des instabilités de falaises. In Programme Interreg II C, 155-205 (in French and in Italian).Lambert, S., Gotteland, P., Nicot, F., 2009. Experimental study of the impact response of geocells as components of rockfall protection embankments. Natural Hazards and Earth Systems Sciences 9, 459-467.

- Lambert, S. and Bourrier, F., 2012. What we learned from rockfall impacts. Workshop Dynamic Rockfall Impacts, Bern, 28 November 2012.

- Lambert, S., Bourrier, F., Toe, D., 2013. Improving three-dimensional rockfall trajectory simulation codes for assessing the efficiency of protective embankments. International Journal of Rock Mechanics and Mining Sciences, Vol. 60, p. 26-36. Doi:10.1016/j.irmms.2012.12.09.
- Lambert, S. and Bourrier, F., 2013 Design of rockfall protection embankments: A review, Engineering Geology, 154, pp 77 – 88, 2013
- Lambert, S., Heymann, A., Gotteland, P., Nicot, F. 2014. Real-scale investigation of the kinematic response of a rockfall protection embankment. Natural Hazards and Earth Systems Science. Vol. 14, p. 1269–1281, Doi: 10.5194/nhess-14-1269-2014.
- Laue, J., Chikatamarla, R., Springman, S., 2008. Do we need coded load assumptions for rockfall protection measures? Proceedings of Interdisciplinary workshop on rockfall protection, Morschach, Switzerland, 55-57.
- Lepert, P., Corté, J., 1988. Centrifuge modeling of the impact of large blocks of rock on a protection structure. Centrifuge 88, Paris, France, 457-465.
- Li, Q., Chen, X., 2003. Dimensionless formulae for penetration depth of concrete target impacted by a non-deformable projectile, Int. J. Impact Eng. 28 (1): pp 93–116.
- Lorentz, J., Plassiard, J-P., Muquet, L., 2010. An innovative design process for rockfall embankments: application in the protection of a building at Val d'Isère. Proceedings of the 3rd Euro Mediterranean Symposium on Advances in Geomaterials and Structures - AGS 2010, Djerba, Tunisia, 277-282.
- Maccaferri, 2009. Rockfall embankments – in Cretaz (Cogne – Aosta), Reinforced soil with the Green Terramesh system, case history, Rev: 01, January 2009.
- Maegawa, K., Tajima, T., Yokota, T., Tohda, M., 2011. Slope-rockfall tests on wall embankments reinforced with geosynthetics. Proceedings of the 6th international structural engineering and construction conference, Zürich, Switzerland, 641-646.
- Mannsbart, G., 2002. Geosynthetic reinforced protection structures in mountainous regions- examples of safe and cost-effective alternatives to conventional structures. Proceedings of the 7th International conference on geosynthetics, Nice, France, 299-301.
- Masuya, H., Amanuma, K., Nishikawa, Y., Tsuji, T., 2009. Basic rockfall simulation with consideration of vegetation and application to protection measure. Natural Hazards and Earth System Sciences 9, 1835-1843.
- Mathieu, Y., Marchal, J., 1989. Déviation de la route nationale 90 à Aigueblanche – Réalisation d'un massif renforcé par géotextile et parement Pneusol: le Pneutex. Bulletin des Laboratoires des Ponts et Chaussées 162, 77-80 (in French)
- Mayne, P.W., Jones, S.J., 1983. Impact stresses during dynamic compaction. Journal of Geotechnical Engineering 109, 1342-1346.
- Mölk, M., Hofmann, R., 2011. The Austrian standard ONR 24810: design of rock-fall protection measures. Partial factor of safety-approach and best practice for the design of rock-fall embankments. Proceedings of Interdisciplinary workshop on rockfall protection – Rocexs 2011, Innsbruck, Austria, 45-46.
- Mölk, M. and Hofmann, R. 2013 Design of rockfall embamkments according to the Austrian ÖNORM rule ONR 24810:2013. 6th Colloquium "Rock Mechanics - Theory and Practice. Vienna.
- Mongiovi, L., Bighignoli, M., Danzi, A. and Recalcati, P. 2014. An impact test on a reinforced earth embankment. Proceedings of Interdisciplinary workshop on rockfall protection - Rocexs 2014, Lecco, Italy,
- Montani, S., 1998. Sollicitation dynamique de la couverture des galeries de protection lors de chutes de blocs. PhD thesis, EPFL Lausanne, Switzerland (in French).
- Morino, A., Grassi, P., 1990. Design and construction of a reinforced earth embankment for protection against rock falls. Proceedings of the 4th International Congress on Geotextiles, Geomembranes and Related Products, The Hague, The Netherlands, 124.

- Murashev, A., Easton, M. and Kathirgamanathan, P., 2013. Advanced numerical modelling of geogrid-reinforced rockfall protection embankments Proc. 19th NZGS Geotechnical Symposium. Ed. CY Chin, Queenstown.
- Nicot, F., Gotteland, P., Bertrand, D., Lambert, S., 2007. Multi-scale approach to geo-composite cellular structures subjected to impact. International Journal for Numerical and Analytical Methods in Geomechanics 31, 1477-1515.
- Oggeri, C., Peila, D., Recalcati, P., 2004. Rilevati paramassi. Proceedings of Convegno Bonifica di versanti rocciosi per la protezione del territorio, Trento, Italy, 191-232 (in Italian)
- ONR, 2013. ONR 24810: Technischer Steinschlagschutz – Begriffe, Einwirkungen, Bemessung und konstruktive Durchbildung, Überwachung und Instandhaltung, ASI Austrian Standards Institute (Österreichisches Normungsinstitut), Ausgabe 15.01.2013.
- Paronuzzi, P., 1989. Criteri di progettazione di rilevati paramassi. Geologia tecnica 1, 23-41 (in Italian).
- Peckover, F.L., Kerr, W.G., 1977. Treatment and maintenance of rock slopes on transportation routes. Canadian Geotechnical Journal 14 (4), 487-507.
- Peila, D., Castiglia, C., Oggeri, C., Guasti, G., Recalcati, P., Sassudelli, F., 2000. Full scale tests on geogrid reinforced embankments for rock fall protection. Proceedings of the 2nd European Geosynthetics Conference and Exhibition, Bologna, Italy, 317-322.
- Peila, D., Oggeri, C., Castiglia, C., Recalcati, P., Rimoldi, P., 2002. Testing and modelling geogrid reinforced soil embankments to high energy rock impacts. Proceedings of the 7th International conference on geosynthetics, Nice, France, 133-136.
- Peila, D., Oggeri, C., Castiglia, C., 2007. Ground reinforced embankments for rockfall protection: design and evaluation of full scale tests. Landslides 4 (3), 255-265.
- Peila, D., 2011. Ground reinforced embankments for rockfall protection: From real scale tests to numerical modelling. In: Lambert, S., Nicot, F. (Eds), Rockfall engineering. John Wiley and Sons, New York, ISTE ltd, London, 393-426.
- Pichler, B., Hellmich, Ch., Mang, H. A., 2005. Impact of rocks onto gravel - Design and evaluation of experiments, International Journal of Impact Engineering 31 pp 559–578.
- Plassiard, J.-P. Modélisation par la méthode des éléments discrets d'impacts de blocs rocheux sur structures de protection type merlons, Phd-Thesis, Sciences de l'ingénieur, Université Joseph-Fourier, Grenoble, 2007
- Plassiard, J.-P., Donzé, F.-V., 2009. Rockfall impact parameters on embankments: a discrete element method analysis. Structural engineering international 19 (3), 333-341.
- Plassiard, J.-P., Donzé, F.-V., 2010. Optimizing the design of rockfall embankments with a discrete element method. Engineering Structures 32 (12), 3817-3826.
- Ploner, A., Sönser, Th., Tropper, W., 2000. Planung von optimierten Steinschlag- und Felssturzschutzmassnahmen, Felsbau, 18, Heft 1.
- Protec Engineering, 2011. www.proteng.co.jp/english/dike_testing.html.
- Rimoldi, P., Lorizzo, R., Pettinau, D., Rocallo, C., Secci, R., 2008. Impressive Reinforced Soil Structures in Italy. Proceedings of the 1st Pan American Geosynthetics Conference, Cancun, Mexico, 789-798.
- Ronco, C., Oggeri, C., Peila, D., 2009. Design of reinforced ground embankments used for rockfall protection. Natural hazards and earth system sciences 9, 1189-1199
- Ronco, C., Oggeri, C., Peila, D., Bertolo, P., Ferraiolo, F., Giacchetti, G., 2010. Numerical modeling of ground reinforced embankments used for rockfall protection. Proceedings of the 3rd Euro Mediterranean Symposium on Advances in Geomaterials and Structures-AGS 2010, Djerba, Tunisia, vol. 2, 269-276.
- Rovina, H., Liniger, M., Jordan, P., Gruner, U., Bollinger, D., 2011. Empfehlungen für den Umgang mit Sturzmodellierungen, Swiss Bull. angew. Geol., Vol. 16/1.

- Simmons, M., Pollak, S., Peirone, B., 2009. High energy rock fall embankment constructed using a freestanding woven wire mesh reinforced soil structure. Proceedings of the 60th Highway Geology Symposium, Buffalo, New York, 290-301.
- Subrin, D., 2006. Modélisation analytique et numérique pseudo-statique des merlons de protection contre les chutes de blocks rocheux. Proceedings of Journées Nationales de Géotechnique et de Géologie, Lyon, France, 145-152 (in French)
- Sung, E., Yashima, A., Aminata, D., Sugimori, K., Sawada, K., Inoue, S., Nishida, Y., 2008. Numerical assessment of the performance of protecting wall against rockfall. Proceedings of the 5th International Symposium on Earth Reinforcement, Kyushu, Japan, 861-867.
- Tissières, P., 1999. Ditches and reinforced ditches against falling rocks. Proceedings of the Joint Japan-Swiss Scientific Seminar on Impact load by rock fall and design of protection structures, Kanazawa, Japan, 65-68.
- Toe, D., Lambert, S., Bourrier, F., Berger, F., 2013. Improving rebound models in 3D rockfall simulation codes used for the design of protection embankments. 8-th International Symposium on Impact Engineering (ISIE2013), Osaka, Japon, 2-4 sept.
- UNI, 2012. UNI 11211-4:2012: Opere di difesa dalla caduta massi - Parte 4: Progetto definitivo ed esecutivo (in Italian).
- Usiro, T.; Kusumoto, M.; Onishi, K.; Kinoshita, K., 2006. An experimental study related to rockfall movement mechanism, Doboku Gakkai Ronbunshu FVOL. 62, No. 2, pp 377-386.
- Wang, B. and Cavers, D.S., 2008. A simplified approach for rockfall ground penetration and impact stress calculations. Landslides, January 2008.
- Willye, D.C., 2014. Rock Fall Engineering. CRC Press. 270 p.
- Whitside, P.G.D., 1986. Discussion on rockfall protection measures. Conference on rock and excavation engineering in an urban environment, Hong Kong, pp 490-492.
- Yoshida, H., 1999. Recent experimental studies on rockfall control in Japan. Proceedings of the Joint Japan-Swiss Scientific Seminar on Impact load by rock fall and design of protection structures, Kanazawa, Japan, 69-78.
- Yoshida, H.; Nomura, T.; Wyllie, D. C.; Morris, A. J., 2007. Rockfall sheds - application of Japanese designs in North America, 1st North American Landslide Conference, June 5th 2007, ♯98205 ASCE.